


1

# Bioremediation of multiple heavy metals through biostimulation of Microbial-Induced Calcite Precipitation at varying calcium-to-urea concentrations

**Authors:** Carla Comadran-Casas [1], Cise Unluer [2], Adrian M. Bass[3], John Macdonald[3], Elmira Khaksar Najafi[1], Caroline Gauchotte-Lindsay[1]

[1] Department of Infrastructure and Environment, James Watt School of Engineering, the University of Glasgow, United Kingdom

[2] Department of Civil Engineering and Management, University of Manchester, Manchester M13 9PL, United Kingdom

[3] School of Geographical & Earth Sciences, University of Glasgow, Glasgow, United Kingdom

Corresponding author: Carla Comadran Casas (Carla.ComadranCasas@glasgow.ac.uk)

Address: Advanced Research Centre, University of Glasgow, 11 Chapel Ln, Glasgow, G11 6EW, Scotland, UK

## Abstract

Studies on heavy metal bioremediation through Microbial-Induced Calcite Precipitation (MICP) typically involve bioaugmentation approaches that use low calcium-to-urea ratios and target single contaminants. We present an investigation on the efficiency of soils' autochthonous ureolytic bacteria to simultaneously remediate multiple heavy metals and sequester carbon through urea hydrolysis and MICP on an urban soil containing excess Pb, Zn, Mn, Sr, Ba and Al and two regional sandy soils. Soils were treated at a fixed urea concentration of 333 mM and increasing calcium content of 0, 50 and 333 mM to provide a range of carbonation potential. Urea hydrolysis ($Ca^{2+}$ = 0 mM) did not produce quantifiable soil carbonation and mobilised Mn into the exchangeable fraction. $Ca^{2+}$ at 50 mM delayed soils' autochthonous ureolytic activity and produced limited carbon and heavy metal mineralisation ($CaCO_3$ = 0-0.7%). 333 mM of $Ca^{2+}$ inhibited urea hydrolysis however, if applied following urea hydrolysis, both carbon ($CaCO_3$ = 4-7%) and heavy metal (Pb, Zn, Mn, Sr and Ba) mineralisation were maximised. Urea hydrolysis and MICP were most successful in removing Pb and Zn from the exchangeable fraction (>85%). However, the higher pH induced by urea hydrolysis at $Ca^{2+}$ = 0-50 mM (~9) compared to 333 mM (~8.5) favoured partition of Pb into the oxyhydroxide fraction. Instead, partition of Zn, Mn, Sr and Ba into the soil carbonate fraction increased with increasing calcium, whilst there was no evidence of Al carbonation. The results of this study evidence the feasibility of biostimulation approaches to remediate multiple contaminants simultaneously through MICP, provide insights into multiple element's behaviour during urea hydrolysis and MICP and demonstrate carbon and element mineralisation are maximised at equimolar calcium-to-urea ratio of 333 mM.

**Keywords**: Biostimulation; MICP; heavy metals; soil remediation; carbon sequestration

## 1. Introduction

Land reclamation, i.e., “ways of restoring ecosystems that have been degraded by human actions such as chemical pollution” (Cuff and Goudie, 2001), is to play a relevant role in the sustainable development of urban areas faced with development pressures. Urban soils contain contaminants, such as trace elements (e.g., Cd, Pb, Cu, Zn, As), radionuclides (e.g., $^{90}Sr$), organic contaminants (e.g., polycyclic aromatic hydrocarbons, polychlorinated biphenyl) and emerging contaminants (e.g., pharmaceuticals, plastics, nanomaterials) (FAO, 2021). Approaches to soil remediation comprise chemical (e.g., oxidation/reduction, electrolysis), physical (e.g., soil washing, grouting, thermal desorption, vitrification) and biological (e.g., biopiles, phytoremediation) methods. Physical and chemical methods can be energy intensive and costly, require substantial resource input and result in loss of land functionality and secondary pollution (Song et al., 2019). In recent years, nature-based solutions (NBS), i.e., “inspired by, supported by, or copied from nature” (Van den Bosch and Sang, 2017) are at the forefront of global efforts due to their environmental, societal, and economic benefits, as recognised by the United Nations 2030 Agenda for Sustainable Development (UN, 2015).

Microbial-Induced Calcite Precipitation (MICP) is a biogeochemical process where microbial activity is stimulated to generate environmental conditions favouring the precipitation of carbonate minerals (i.e., abundance of carbonate ions and alkaline environment – pH ≥8.5). Several microbial processes are known to result in MICP (e.g., ammonification, denitrification, sulphate and iron reduction). Ammonification of urea, or ureolysis, has been the most widely investigated approach due to its easiness to induce and monitor, simple nutritional requirements (Lapierre et al., 2020), rapid response, ubiquitousness of ureolytic bacteria (Burbank et al., 2012) and robustness against environmental conditions (e.g., oxic/anoxic conditions, high salt content, wide temperature range, soil types, climates, and acid/alkaline conditions) (Mitchell, and Santamarina, 2005; Mortensen et al., 2011; Stabnikov et al., 2013; Cheng et al., 2014; Helmi et al., 2016; Kim et al., 2018). In this approach, bacteria use the urease enzyme to catalyse the hydrolysis of urea into ammonia and carbamide (1). Carbamide spontaneously hydrolyses into ammonia and carbonic acid (2), which subsequently equilibrate with water as bicarbonate and ammonium ions (Eqs. (3) and (4). The excess of hydroxide ions between pH 6.3 and 9.3 ($pK_1$ and $pK_a$, respectively) results in a net increase in pH, in turn producing carbonate ions. Given the presence of calcium ions, this leads to the precipitation of calcium carbonate minerals (5) (Gat and Tsesarsky, 2017).

$$CO(NH_2)_2 + 2H_2O \xrightarrow{urease} NH_3 + NH_2COOH \quad (1)$$

$$NH_2COOH + H_2O \rightarrow NH_3 + H_2CO_3 \quad (2)$$

$$H_2CO_3 \leftrightarrow H^+ + HCO_3^- \quad (3)$$

$$2NH_3 + 2H^+ \leftrightarrow 2NH_4^+ + 2OH^- \quad (4)$$

$$Ca^{2+} + HCO_3^- + OH^- \leftrightarrow CaCO_3 + H_2O \quad (5)$$

During MICP, toxic species of heavy metals (e.g., $Pb^{2+}$) can be mineralised through isomorphous substitution of calcium ($Ca^{2+}$) or co-precipitate as carbonates (e.g., $PbCO_3$). Carbonation of toxic elements decreases their bioavailability and thus the potential to result in harmful effects to living organisms (Sardar et al., 2013). Accordingly, MICP has been investigated for its bioremediation potential of heavy and transition metals in various media, including soil, water, mine tailings, slag, and wastewater sludge. Bioremediation experiments on MICP treated soils contaminated with toxic heavy metals metals consistently show removal of >97% $Cr^{6+}$ (Chat et al., 2009; Achal et al., 2013; Kumari et al., 2014;), 96.6% $As^{3+}$ (Achal et al., 2012a), 26-86% $Pb^{2+}$ (Achal et al., 2012b; Govarthanan et al., 2013; Yang et al., 2016; Liu et al., 2021), 80% $Sr^{2+}$ (Achal et al., 2012c), 13-88% $Cd^{2+}$ (Govarthanan et al., 2013; Liu et al., 2021), 96% $Ni^{2+}$ (Zhu et al., 2016), 92-97% $Cu^{2+}$ (Govarthanan et al., 2013; Chen and Achal, 2019) and 21-66% $Zn^{2+}$ (Liu et al., 2021) from the soluble/exchangeable soil fraction, accompanied by respective increases in the soil carbonate-bound fraction, thereby showing potential as a bioremediation technique.

The effect of fundamental factors affecting the efficiency of bioremediation via MICP are still unclear and are being investigated. In particular, the presence of $Ca^{2+}$ along with toxic elements during MICP has been found to both favour (Bhattacharya et al., 2018; Fang et al., 2021) and hinder (Chung et al., 2020) microbial activity. In a study on $Cd^{2+}$, $Ca^{2+}$ was shown to protect the cell by lowering the environment pH and competing with the $Cd^{2+}$ on the cell surface, thereby decreasing toxic element adsorption onto the cell surface (biosorption) and its toxicity (Fang et al., 2021). However, increased concentration of $Cu^{2+}$ in soil due to exchange with $Ca^{2+}$ has been reported to result in increased toxicity (Chung et al., 2020). Another critical role of $Ca^{2+}$ in MICP is the control the extent of soil carbonation, which directly affects soil mechanical properties (e.g., permeability, shear strength, liquefaction) and could prove desirable in urban settings. Calcium chloride has been shown to induce higher urease activity and calcite precipitation over other calcium sources (Achal et al., 2014). MICP applications in soil engineering typically use a calcium-to-urea ratio of 333:333 mM after Al Qabany et al. (2012) to maximise carbonation and enhancement of mechanical properties. Bioremediation studies have typically used lower calcium-to-urea molar ratios (25:333 mM) which have shown to be sufficient for the carbonation of toxic elements (Achal et al., 2012a; 2012b; 2012c; Kumari et al., 2016; Yang et al., 2016; Zhu et al., 2016; Chen and Achal, 2019). However, the low calcium-to-urea molar ratio limits the potential for both carbon sequestration through mineral trapping and improvement of soil mechanical properties. In agricultural settings, the application of urea as a fertiliser is common and typically excludes $Ca^{2+}$. In this case, urea hydrolysis may result in carbon sequestration through

solubility trapping rather than mineral trapping, and bioremediation of toxic elements through non-calcium-based carbonate minerals (e.g., $PbCO_3$). Thus, the effect of varying calcium-to-urea ratios may result in differing bioremediation efficiencies and carbon sequestration mechanisms, leading to variations in carbonate products and physical properties of soil.

In practice, there are still important aspects that hinder the applicability of MICP as a bioremediation technique. One aspect is that most research has been conducted on bioaugmentation (Chai et al., 2009; Achal et al., 2012a; 2012b; 2012c; 2013; Govarthanan et al., 2013; Kumari et al., 2014a; 2014b; Yang et al., 2016; Zhu et al., 2016; Chung et al., 2020; Liu et al., 2021) as opposed to biostimulation (Chen and Achal, 2019; Lyu et al., 2022). Bioaugmentation has the drawback of increasing treatment costs and introducing exogenous bacteria, which suffer predation once introduced in the soil environment (Burbank et al., 2012). Furthermore, culturable bacteria represent a very low amount (est. <1%) of soil total bacteria diversity (Youseif et al., 2021), hence capturing a very small proportion of the soils' genetic pool potential for self-remediation. Biostimulation of indigenous bacteria can offer several advantages over bioaugmentation. Chen and Achal (2019) and Lyu et al. (2022) showed carbonation of $Cu^{2+}$ and $Cd^{2+}$ through biostimulation, evidencing its plausibility as a bioremediation approach. Minimal inhibitory concentrations (MIC) of ureolysis vary across elements and ureolytic bacteria species and, despite growth slowdown to inhibition is consistently observed with increasing concentration of $Cu^{2+}$(Achal et al., 2011; Mugwar and Hardbottle, 2016; Kim et al., 2021), $As^{3+}$ (Achal et al., 2012a), $Cd^{2+}$ (Kang et al., 2014; Mugwar and Harbottle, 2016; Kim et al., 2021;) and $Pb^{2+}$ (Mwandira et al., 2017; Mugwar and Harbottle, 2016; Zhao et al., 2017; Jiang et al., 2019; Kim et al., 2021), autochthonous ureolytic consortiums may be better adapted to local pollutant conditions than exogenous bacteria. In the context of geotechnical engineering, no specific benefits of bioaugmentation over biostimulation have been observed with respect to microbial activity, resulting environmental conditions, and enhancement of soil mechanical properties (Gomez et al., 2017). Additionally, indigenous bacteria could minimise heterogeneity of calcite precipitation in soil produced by an uneven distribution of injected bacteria. Another factor hindering applicability of MICP is that studies on soils affected by multiple contaminants are still scarce (Govarthanan et al., 2013; Yang et al., 2016; Liu et al, 2021) and, to our knowledge, limited to bioaugmentation. In presence of multiple toxic elements, element atomic radii and valence could play a role in the specificity for element carbonation. In particular, divalent elements may combine with carbonate ions ($CO_3^{2-}$) more easily (He et al., 2019), while elements with smaller atomic radii than $Ca^{2+}$ (i.e., $Pb^{2+}$, $Zn^{2+}$, $Li^{2+}$, $Cr^{6+}$, $Mn^{2+}$, $Cd^{2+}$, $Co^{2+}$, $Ni^{2+}$, $Cu^{2+}$, $Ni^{2+}$) may be more easily incorporated in the calcium carbonate mineral structure than elements with a larger atomic radius (i.e., $Sr^{2+}$, $Ba^{2+}$) which could lead to differing bioremediation efficiencies across elements.

The current state of art highlights the need to advance knowledge on the bioremediation efficiency of MICP through biostimulation in the presence of multiple toxic elements, considering the different heavy metal immobilisation mechanisms and additional ecosystem services (e.g., soil stabilisation, carbon sequestration). To this end, the first goal of this study was to determine whether MICP through biostimulation of autochthonous ureolytic bacteria could be induced in the presence of multiple toxic

elements. The second goal was to assess the bioremediation efficiency under varying calcium-to-urea molar ratios to maximise concomitant heavy metal and carbon sequestration through mineral trapping. The calcium-to-urea molar ratios covered a range of scenarios in which MICP may occur—i.e., agricultural, bioremediation and engineering—under the hypothesis of increased bioremediation efficiency and carbon sequestration through mineral trapping with increasing calcium content. The obtained results provided scientific evidence on the biostimulation of autochthonous ureolytic bacteria for the simultaneous bioremediation of multiple toxic elements and carbon sequestration through mineral trapping.

## 2. Materials and Methods

### 2.1. Soil sampling

The soils used in this study comprised two sandy soils from quarries and a soil from a vacant and derelict land site in Glasgow (Figure 1). Reddish and yellow sand samples were sourced from Garnock (GQ) and Hullerhill (HQ) quarries, respectively, operated by Hugh King & Co and located in Ayrshire, Scotland (UK) (GQ: 55.63757713, -4.718350936; HQ: 55.66784963, -4.66816856; WGS84). The soil sample from the vacant and derelict site (GLA) was obtained from Glenconner Park (Glasgow, Scotland, UK, Figure S 1). The top ~40 cm soil profile revealed a top organic layer of soil overlaying a brown/reddish clay layer (Figure S 1). An interbedded layer of made ground consisting of non-cohesive granular material of sandy to gravelly texture with fines and of light to dark colour was sampled, where bricks and unidentified rubble were appreciable. Once in the laboratory, soil samples were sieved <2 mm in sterile conditions and stored in a cooled room at 4°C until further use. A subsample from each soil was analysed for particle size distribution, total carbon, total and exchangeable elemental composition and mineralogy as specified in Section 2.5.

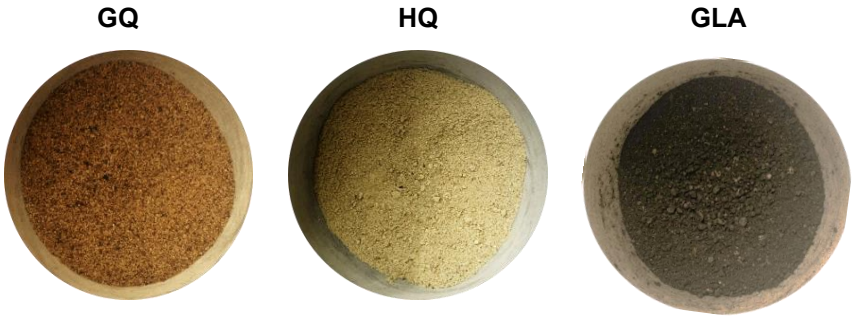


**Figure 1 Reddish sand from Garnock quarry (GQ), yellow sand from Hullerhill quarry (HQ), Ayrshire, and sandy soil from vacant and derelict land site in Glenconner park, Glasgow, (GLA).**

### 2.2. Treatment solutions

MICP solution treatments contained 333 mM urea (Fisher Scientific, ≥99.5% ACS reagent), 10 g/L ammonium chloride ($NH_4Cl$, VWR Chemicals, ≥99.9% ACS reagent), 3 g/L nutrient broth (Sigma Aldrich) and either 0-, 50-, or 333-mM calcium chloride dihydrate ($CaCl_2 \cdot 2H_2O$, Sigma Aldric, ≥99%

ACS reagent) in deionised water (Milli-Q water filtration system Elga Purelab Chorus). Control treatments were equally prepared but excluded urea. Stock solutions were filter sterilised through sterile 0.2 µm syringe filters (Sartorius Minisart), transferred into pre-autoclaved glass bottles in sterile conditions and stored at 4ºC until further use.

## 2.3. Application of MICP treatments

Samples were prepared by adding 2 g of soil (<2 mm) in sterile DNA, DNAse, RNAse free15 mL centrifuge tubes (Sarstedt AG&Co KG). Following preparation, 4 mL treatment solution was pipetted, tubes were closed and thoroughly shaken to mix soil and solution, which marked $t$ = 0. Both sample preparation and treatment application were conducted in sterile conditions. Samples were subsequently transferred into an orbital shaker incubator set at room temperature (20±3ºC) and gentle shaking (150 rpm) and allowed to react in closed vials and dark conditions.

MICP treatments comprised one stage treatments, where treatment solution was applied once, and two stage treatments, where treatment solution replacement occurred once after a certain reaction time. One stage treatments comprised: urea with 0 mM $Ca^{2+}$ (U); urea with 50 mM $Ca^{2+}$ (U LCa); urea with 333 mM $Ca^{2+}$ (U HCa); and their respective controls without urea: C, C LCa, C HCa. Samples were taken at reaction time points ($t_r$) 1 h, 1, 2, 3 and 4 d. For samples in which no significant increase in solution pH was observed within this time period (indicative of no ureolysis), reaction time was extended up to 20 d. Two-stage treatments comprised treatment cases containing high calcium, i.e., urea with 333 mM $Ca^{2+}$ (U HCa 2S) and its respective control (C HCa 2S). For these two treatments, an initial application of 4 mL of either U or C treatment solution was allowed to react for $t_r$ = 4 d. This was followed by solution replacement and application of 4 mL of either U HCa or C HCa treatment solution which was allowed to react for $t_r$ = 1 d, making a total of a 5-d treatment. To replace the treatment solution, samples were centrifuged at 5000 rpm for 20 min. Then, in sterile conditions, the supernatant was decanted, and fresh treatment solution was pipetted as previously detailed. Sampling was destructive and three replicate samples were prepared for each time point and treatment.

## 2.4. Post-treatment sampling

Following reaction time, 15 mL tubes containing soil and treatment solution were centrifuged at 5000 rpm for 20 min. In sterile conditions, the supernatant was decanted, filtered through sterile 0.2 µm syringe filters, transferred into 2 mL pre-autoclaved centrifuge tubes, and subsequently stored at -20ºC until analysis of solution pH (see Section 2.5.1). The remaining soil samples were stored at -20ºC for post-treatment geochemical characterisation. In preparation for geochemical analyses, soil samples were oven dried at 70ºC to a constant mass. Soil sample replicates were gently homogenised with a pestle and mortar to produce a composite sample. Three 1 g subsamples were then obtained for sequential extraction of heavy metals (see Section 2.5.4). The remaining composite sample was ground and sieved <50 µm in preparation for XRD and TG analyses (see Section 2.5.5 and 2.5.6, respectively).

## 2.5. Physicochemical analyses

### 2.5.1. pH

Solution pH was analysed with a pH meter (Orion Star A215, Thermo Scientific) probe (Orion ROSS Ultra SM 103BNUWP, Thermo Scientific), calibrated to three points (pH = 4, 7 and 10, Orion Application Solution, Thermo Scientific).

### 2.5.2. Particle size distribution

Soil samples were oven dried at 105ºC to a constant mass and subsequently pre-treated with hydrogen peroxide on a hot plate at 90°C to remove soil organic matter. The particle size distribution (PSD) of the mineral soil fraction was analysed on three replicate samples with a laser diffractometer (Bettersize 2600 Laser Particle Analyzer, BT-802, Bettersize Instruments Ltd.).

### 2.5.3. Soil total carbon

Soil total carbon of three replicate samples were analysed with a Picarro Combustion Module Cavity Ring-Down Spectroscopy (CM-CRDS) system (CM by NC Technologies, G2201-i CDRS) interfaced by a Caddy Continuous Flow Interface (A2100).

### 2.5.4. Soil elemental composition and heavy metal partition into soil fractions

The total elemental composition of untreated soil samples was carried out through a triacid (HF, $HNO_3$ and HCl) digestion on a hotplate at the Scottish University Environment Research Centre (SUERC, East Kilbride, G75 0QF, Scotland, UK) on three replicate samples from each soil. The triacid digestion consisted of digesting the soil samples overnight on a hotplate at 120º consecutively, first with Hf+$HNO_3$, secondly with $HNO_3$ and finally with HCl, drying the sample in between the applied solutions. Elements were determined by inductively coupled plasma-optical emission spectrometry (ICP-OES, Thermo Scientific iCap 7000) or ICP-mass spectrometry (ICP-MS, Agilent 7500ce). The element partition into soil exchangeable, carbonate, organic matter, oxyhydroxide and residual fractions was determined through sequential extraction (Tessier et al., 1979).

The exchangeable and carbonate extraction steps were conducted on treated samples obtained after $t_r$ = 1 h, 1, 4 and 5 d. The organic matter, oxyhydroxide and residual extraction steps were conducted on samples treated with the U treatment at $t_r$ = 1 h, and samples treated with U HCa and U LCa at $t_r$ = 4 d. The residual fraction was conducted though a triacid digestion at SUERC as previously mentioned. Elements Na, K, Mg, Ca, Sr, Ba, Ti, V, Cr, Mo, Mn, Fe, Co, Ni, Cu, Zn, Cd, B, Al, Si, Sn, Pb, As, Sb, S, Se on samples obtained from extraction steps 1-4 were determined by ICP-OES (Agilent 5900 SVDV). These same elements were determined by ICP-OES (Thermo Scientific iCap 7000) or ICP-mass spectrometry (ICP-MS, Agilent 7500ce) at SUERC following extraction step 5.

### 2.5.5. Powder X-Ray Diffraction (XRD)

The mineralogy of ground (<50 µm) soil samples was analysed by powder X-ray diffraction. X-ray diffraction patterns were collected at ambient temperature on a Malvern Panalytical Empyrean with

PIXcel3D-Medipix3 1x1 detector using Cu Kα radiation (wavelength 1.541874 (Å)). Data were collected in Bragg-Brentano reflection geometry 5-80° 2θ, step size 0.0131°. Data analysis was carried out with the HighScore Plus software (version 5.1a 5.1.1.30138, Malvern Panalytical B.V., Almelo, the Netherlands). Rietveld refinement was used to quantify soil mineralogy.

### 2.5.6. Thermogravimetric analysis

The thermal decomposition of soil samples collected at $t_r$ = 1 h, 1, 4 and 5 d and chemicals used in treatment solutions (i.e., urea, calcium chloride dihydrate, nutrient broth and ammonium chloride) were analysed with a thermogravimetric analyser (TGA 8000, PerkinElmer). Samples of 10-15 mg weight were heated from 30 to 1100ºC at a rate of 10ºC/min. $N_2$ was used as a carrier gas, with sample and balance purges set to 40 and 60 mL/min, respectively. Data analysis was carried out with the Pyris software (Pyris™ V13.4.0, PerkinElmer).

## 2.6. Data analysis

The statistical package R (v. 4.2.2) (Wickham, 2016; de Mendiburu, 2021; R Core Team, 2022) was used to compute average and standard deviation of replicate samples (e.g., pH, PSD, TOC) and analyse the data derived from the sequential extraction. A non-targeted hierarchical cluster analysis (HCA) was used to elucidate similarities in elements behaviour caused by treatment and reaction time in the soil exchangeable and carbonate fractions. The R packages 'dendextend', 'factoextra', 'cluster', 'pheatmap' and 'NbClust' were used for HCA.

The element concentrations from the sequential extraction at $t_{end}$ were normalised with respect to samples treated with control treatment (C) at $t_0$ ($t_r$ = 1 h) to remove the effect of applied chemicals other than urea and $CaCl_2$. The normalised averages and error propagated during normalisation at $t_0$ and $t_{end}$ for each element were computed as:

$$t = 0 \qquad E_{n,0} = \frac{E_{0,av}}{E_{0,av}}\left(1 \pm \sqrt{2}\,\frac{E_{0,sd}}{E_{0,av}}\right) = 1 \pm \sqrt{2}\,\frac{E_{0,sd}}{E_{0,av}} \tag{6}$$

$$t = end \qquad E_{n,f} = 1 - \frac{E_{f,av}}{E_{0,av}}\left(1 \pm \sqrt{\left(\frac{E_{0,sd}}{E_{0,av}}\right)^2 + \left(\frac{E_{f,sd}}{E_{f,av}}\right)^2}\right) \tag{7}$$

Where $E_{n,0}$ and $E_{n,f}$ are the normalised average concentrations of element '$E$' and subscript '0' and 'f' indicate reaction time $t_0$ and $t_{end}$, respectively. $E_{0,av}$ and $E_{f,av}$ are average element concentrations and $E_{0,sd}$ and $E_{f,sd}$ their respective standard deviations. Note the normalised element concentration at $t_{end}$ is computed as one minus fraction, therefore positive results would indicate removal and negative results relative increases. Scripts are available upon request.

# 3. Results and Discussion

## 3.1. Pre-treatment soils characterisation

The particle size distribution (Figure S 2 and Table S 1) indicated the GQ and HQ quarry soils were composed of 100% and 90% sand, respectively. The yellow sand (HQ) contained ~9% fines (<63 μm), of which ~2% were of clay size (<2 μm). XRD analysis indicated the main mineral constituents of the GQ soil were quartz (88%) and albite (8.1%), with traces of dolomite, microcline, and enstatite (Table S 4). The HQ soil contained quartz (91%) and kaolinite (8.4%) and traces of muscovite (Table S 5). The GLA soil was a silty sand, with ~31% fines of which <5% were of clay size. The GLA soil mineralogy was quartz (54%), mullite (24%) and bytownite (20%) with traces of birnessite (Table S 6). HQ and GQ soils contained no quantifiable carbon whilst the total carbon in GLA soil samples was determined at 3% (Table S 2). XRD analysis indicated no detectable calcite in any of the soils prior to treatment (Table S 4, 5 and 6).

Total elemental analysis indicated HQ and GQ soils contained Ba, Cr, Cu, Mn, Ni, Pb, Sr, V, Zn <50 mg/kg, except for Ba and Mn in HQ soil which were 50-100 mg/kg, and elements As, Cd, Co, Mo, Sb, B, Li, Sn were <10 mg/kg. The GLA soil contained a significantly higher content of Ba, Mn, Sr and V (>300 mg/kg), Ni and Pb (>200 mg/kg), Cr, Cu and Zn (≥100 mg/kg), Co, Li and As (20-60 mg/kg) and a similar concentration of Cd, Mo, Sb, B and Sn (≤10 mg/kg) (Figure S 3). The main elements in the exchangeable fraction of GLA soil were Al, Ba, Mn, Pb and Zn, determined between 9 to 35 mg/kg, whilst in HQ and GQ soils were <5 mg/kg (Figure S 4a). The rest of elements analysed (As, Cd, Co, Cu, Cr, Mo, Ni, Sb, V) were in trace concentrations (<2 mg/kg) in all three soils (Figure S 4b).

## 3.2. Activity of soil autochthonous ureolytic microorganisms

Soil-solution pH was used as a proxy to monitor the activity of soils' autochthonous ureolytic microorganisms. pH has been routinely used to evidence urea hydrolysis in bioremediation studies in inoculated solutions (Fujita et al., 2000; 2004; Mugwar and Harbottle, 2016; Bhattacharya et al., 2018; He et al., 2019; Do et al., 2020; Kim et al., 2020; Bai et al., 2021; Ali et al., 2022; Xue et al., 2022) , soils (Zhao et al., 2019; Chung et al., 2020; Lyu et al., 2022), mine tailings (Yang et al., 2016; Mwandira et al., 2017; Yin et al., 2021; Proudfoot et al., 2022) and sludge (Zeng et al., 2023). Most importantly, pH indicates favourable conditions for soil carbonation (pH >8.5). Increases in soil solution pH in MICP via urea hydrolysis occur as a result of urea derived $NH_3$ protonation to $NH_4^+$, which generates excess $OH^-$ according to Eqs. (3) and (4). This is favoured increase of pH up to circa 9 when pH is then buffered due to deprotonation of $NH_4^+$ to $NH_3$ ($pK_a$ = 9.26) and $HCO_3^-$ to $CO_3^{2-}$ ($pK_a$ = 10.34). Consistent with urea hydrolysis reactions and pH increases reported in the literature, the application of treatments containing urea and $Ca^{2+}$ ≤50 mM (U, U LCa) to HQ, GQ and GLA soils resulted in increases in soil solution pH to 9 within 2 to 3 days compared to control treatments (C, C LCa) where pH remained <7 (Figure 2a-c), indicating successful biostimulation of urea hydrolysis by soils' autochthonous ureolytic bacteria.

With the application of urea and no calcium (U), the GLA and GQ soils showed a faster increase in soil-solution pH compared to the HQ soil, which could be related to the presence of kaolinite clay. Clay particles can adsorb $OH^-$ ions onto surface positively charged sites (Diamond et al., 1966), limiting increases in soil-solution pH. Bacteria interact physically and chemically with clay particles due to their similar size (bacteria: 0.5-3 µm; clay: ≤2 µm) and surface electrical charges and their metabolic activity can adversely be affected by clays (Mitchell and Santamarina, 2005; Cardoso et al., 2023). Furthermore, clays can adsorb extracellular enzymes, resulting in slower bulk reaction rates (Gianfreda et al., 1992). These factors could have resulted in the observed slower increase in soil solution pH in HQ soil.

With the addition of 50 mM $Ca^{2+}$ (U LCa), increase in soil pH circa 9 was delayed up to 24 h and stabilised at a slightly lower pH (8.8-9) compared to the U treatment (9-9.1) (Figure 2a-c). These effects were more pronounced in the HQ and GLA soils than in GQ. With the addition of 333 mM $Ca^{2+}$ (U HCa), no notable increase in pH could be observed within 4 d, indicating no urea hydrolysis. This was consistently observed across the three soils (Figure 2a-c) and sustained for at least 20 d (GLA, Figure 2d; HQ and GQ, Figure S 6), indicating that 333 mM $Ca^{2+}$ inhibited urea hydrolysis. Urea hydrolysis inhibition by calcium is considered to occur due to increased salinity, causing osmotic stress, and coating of cell surfaces by calcium ions (Fu et al., 2023). In pure cultures of *S. pasteurii*, inhibition has been reported to being at $Ca^{2+}$ >10 mM and completely inhibit urea hydrolysis at 200 mM (Cui et al., 2022). Inoculated in non-contaminated sand, however, urea hydrolysis by *S. pasteurii* has been observed at much higher concentration of up to 1 M $CaCl_2$ (Al Qabany and Soga, 2014). Similarly to this study, autochthonous ureolytic microorganisms in a Cd-seleniferous soil (Cd ~ 10 mg/kg) exhibited slower urea hydrolysis rates when exposed to urea plus calcium (2 and 1 g/kg) compared to solely urea (2 g/kg) (Lyu et al., 2022).

Urea hydrolysis inhibition by monovalent and divalent elements other than calcium may have also contributed to slower urea hydrolysis rates. The order of elements to inhibit soil bulk ureolytic activity at 5 µmol/g were reported to follow the order $Ag^+ \geq Hg^{2+} > Cu^{2+} > Cd^{2+} > Zn^{2+} > Sn^{2+} > Mn^{2+}$ and additional inhibition was observed with $Ni^{2+}$, $Co^{2+}$, $Pb^{2+}$, $Ba^{2+}$, $As^{3+}$, $Cr^{3+}$, $Al^{3+}$, $V^{4+}$ and $Mo^{6+}$ (Tabatabai, 1977). The total concentration of the main elements found in the exchangeable fraction of the GLA soil (Pb, Zn, Mn, Sr, Ba and Al) was of 1.38 µmol/g hence, a level of inhibition in this soil was conceivable. Exchange of calcium ions by adsorbed toxic elements may have additionally contributed to increased toxicity, as observed in a Cu-spiked soil inoculated with *S. pasteurii*, where urea hydrolysis declined with increasing $Ca^{2+}$ to 450 mM and was attributed to Cu-induced toxicity which concentration in solution increased linearly with increasing calcium application (Chung et al., 2022).

Ureolytic bacteria exhibit varying tolerances to toxic elements (Table 1). Elements in the exchangeable fraction prior to treatment were determined at lower concentrations than reported inhibitory bulk values (Tabatabai, 1977) and minimum inhibitory concentrations (MIC) (Table 1). Furthermore, HQ and GQ soils contained significantly lower concentration of potentially toxic elements and differences in the time required to increase soil pH to ~9 between HQ and GQ soils and the GLA soil were not significantly different (Figure 2a-c). This suggested that elements present at the

concentrations determined, nor their combined effect, had a notable negative impact on urea hydrolysis and the observed delay to inhibition with application of 333 mM $Ca^{2+}$ could be largely attributed to calcium.

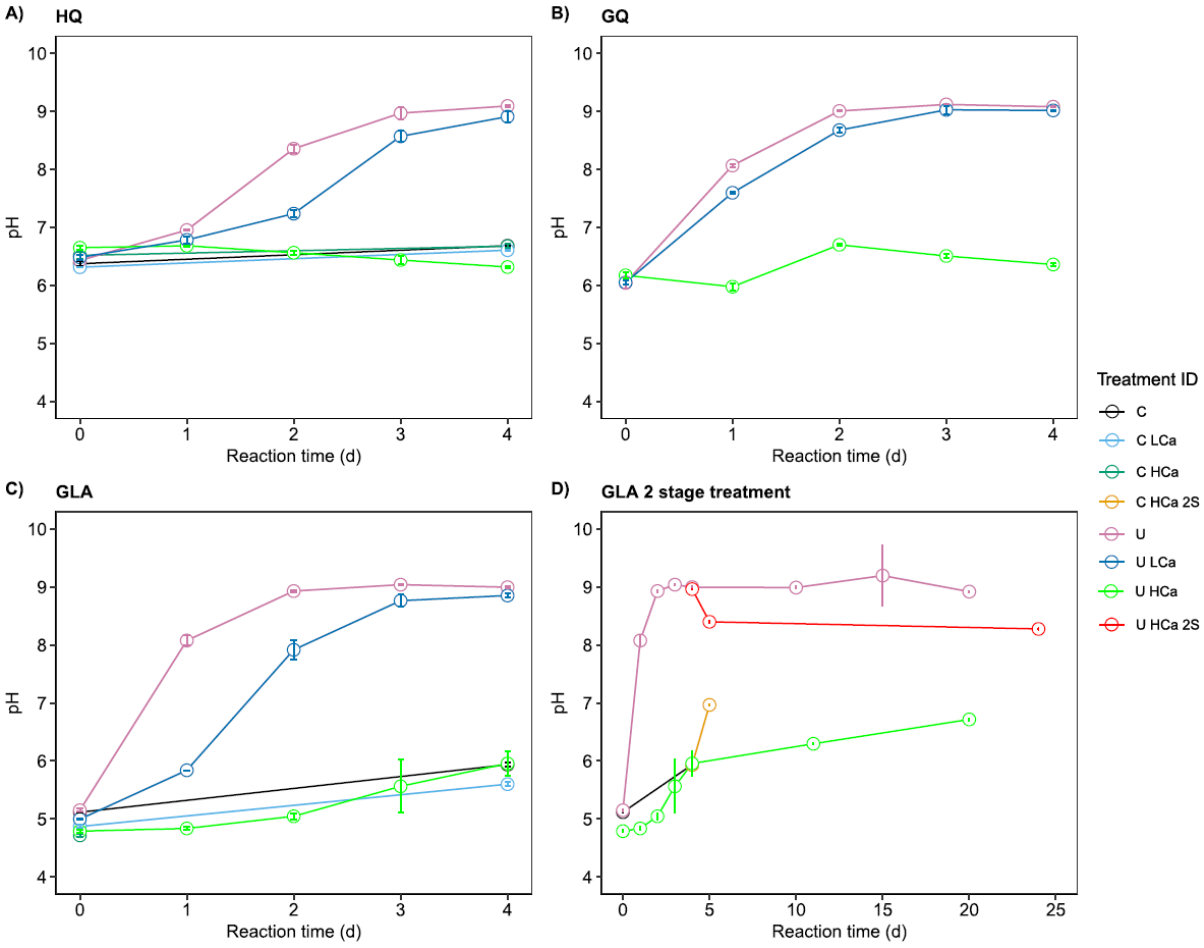


**Figure 2 pH of soil leachates of quarry sands (HQ and GQ) and VDL site soil (GLA) silty sand as a function of reaction time for various soil treatments. Markers and error bars indicate average and standard deviation, respectively, of three replicate samples.**

**Table 1 Minimum inhibitory concentration (MIC) of heavy metals on urea hydrolysis by some elements reported in the literature and present in the GLA soil.**

| Element | MIC (mM) | Microorganism | Ref. | Soils used in this study | | |
|---|---|---|---|---|---|---|
| | | | | GQ (µM) | HQ (µM) | GLA (mM) |
| Pb | 0.01-0.5 | *Pararhodobacter sp.* | Mwandira et al. (2017) | <LoQ (0.01) | <LoQ (0.01) | 0.080±0.003 |
| | 0.97-1.45 | *Bacillus sp. JX910224* | Govarthanan et al. (2013) | | | |
| | 1-30 | *S. pasteurii* | Mugwar and Harbottle (2016); Jiang et al. (2019) | | | |

| | | | | | | |
|---|---|---|---|---|---|---|
| | 100 | *E. cloacae* KJ-46 and KJ-47 | Kang et al. (2015) | | | |
| Zn | 0.2-0.5 | *S. pasteurii* | Mugwar and Harbottle (2016) | <LoQ (0.006) | 4.0±0.6 | 0.130±0.003 |
| | 2.29-3.06 | *Bacillus sp. JX910224* | Govarthanan et al. (2013) | | | |
| | 0.92 | *Sporosarcina* kp-4 and kp-22 | Qiao et al. (2021) | | | |
| Mn | <50 | *S. pasteurii* | Fang et al. (2021) | 1.0±0.6 | 8.0±0.5 | 0.18±0.01 |
| Sr | 2.5-5 | Halomonas sp. | Achal et al. (2012c) | 7.0±0.6 | 3.00±0.07 | 0.080±0.002 |

Urea hydrolysis inhibition by 333 mM $Ca^{+}$ was circumvented with a two-step treatment (Figure 2d). Application of 333 mM $Ca^{2+}$ following 4 d of U treatment and replacement with U HCa treatment for 1 d (U HCa 2S) resulted in increase in pH to 9 on day 4 followed by a decrease to 8-8.5 on day 5, which then remained stable up to 20 days (Figure 2d). With availability of calcium and carbonate ions and a pH >8.5, precipitation of calcium carbonate minerals occurs according to Eq. (5). The observed pH decreased from day 4 to 5 was consistent with pH evolution during MICP (Dupraz et al., 2009) and was indicative of calcium carbonate precipitation. In the corresponding control treatment (C HCa 2S), an increase in pH occurred following application of 333 mM $Ca^{2+}$, which remained ≤7. Studies on the effect of $CaCl_2$ or $NH_4Cl$ application on soil pH have typically reported decreases in pH with salt application (Khonje et al.,1984; Petrie et al., 1984; Sumner, 1994; Kissel et al., 2009) which is attributed to a variable charge mechanism of $Ca^{2+}$ exchange with $H^{+}$ and $Al^{3+}$ adsorbed to organic matter and/or clays (Bache, 1984; Sumner, 1994) and has been observed in the context of MICP (Lyu et al., 2022). However, in highly weathered acidic soils with low organic matter content, $Cl^{-}$ exchange for $OH^{-}$ adsorbed to colloid surfaces may exceed exchange of $Ca^{2+}$ with $H^{+}$ and $Al^{3+}$, resulting in a pH increase with increasing salt content (Sumner, 1994). This could explain the slight increase in soil pH following $CaCl_2$ application in this study, which has also been observed on an acidic soil of similar initial pH (pH = 5.25) (Li et al., 2022).

### 3.3. Effect of $Ca^{2+}$ on soil carbonation

Mineralogical analysis of crystalline components by XRD in GLA soil samples indicated nearly identical patterns for control samples (C, C LCa, C HCa 2S) and samples that received urea and urea-high calcium (U and U HCa) treatments (Figure 3a). No differences in soil mineralogy were detectable between these samples at reaction times $t_0$ and $t_{end}$. Some variability in peak intensities was observable between 2θ = 27 to 28.5, which were attributed to small changes in plagioclase content (Figure 3a). These results confirmed application of control treatments excluding or including calcium, urea hydrolysis with no calcium addition, or where urea hydrolysis was inhibited by high calcium dose, did not result in quantifiable soil carbonation nor other changes in soil mineralogy.

The application of the U HCa 2S treatment to GLA soil samples resulted in two new mineral phases, identified as calcite and salammoniac (identified as “C” and “SA” in Figure 3). Samples that received the U LCa treatment showed an increased peak intensity that coincided with calcite main peak ($2\theta$ = 29.43) (Figure 3b) however, the rest of calcite peaks were hardly observable, and results were inconclusive. Calcite peaks were determined at $2\theta$ equal to 29.43, 48.52, 47.5, 43.15, and 23.1, while other calcium carbonate polymorphs were not detectable. Calcite has been reported as the main carbonate mineral following bioaugmentation of a Pb-contaminated soil (Achal et al., 2012b) and mine tailings (Govarthanan et al., 2013; Yang et al., 2016), although vaterite and aragonite have been additionally identified (Achal et al., 2012b; Govarthanan et al., 2013). Carbonate minerals other than calcite were not detectable with any treatment. However, formation of Pb, Zn, Cu, Cd, Ni and Co carbonate minerals through urea hydrolysis is possible (Kang et al., 2014; 2015; Li et al., 2013; 2016; Zhao et al., 2017; Qiao et al., 2021). With the addition of calcium, Pb, Zn, Cd incorporation into calcite is reported instead, except for Sr which is reported to form a soil-solution of calcian-strontianite (Fujita et al., 2004; Achal et al., 2012b; Govarthanan et al., 2013; Yang et al., 2016; Mwandira et al., 2017; Kim et al., 2021). Thus, soil carbonation may have occurred with the U and U LCa treatments, but the low concentration of divalent elements may have produced carbonation levels below limit of detection. Salammoniac, or ammonium chloride, is a soft halide mineral with formula $NH_4Cl$, soluble in water (39.5 g/100 g water at 25ºC) (Haynes, 2015). Its precipitation with the U HCa 2S treatment was attributed to additional of $Cl^-$ from high calcium chloride dose of 333 mM and excess $NH_4^+$ derived from urea hydrolysis to the already applied $NH_4Cl$. Evidence of ammonium-based minerals was reported by Govarthanan et al. (2013) and Yang et al. (2016), who identified gwihabaite, $(NH_4,K)NO_3$, following MICP treatment.

The observed results in GLA soil were reproducible in GQ and HQ soils, as shown in Figure 3c-d which evidenced calcite and salammoniac precipitation resulted from U HCa 2S treatment. On these soils, increases in calcite peak intensities were unequivocally detectable with the U LCa treatment. As observed in GLA, urea hydrolysis (U) on its own did not result in soil carbonation. The calcite content estimated through Rietveld analysis indicated the U HCa 2S treatment resulted in 6.9, 3.1 and 4.6% calcite in GLA, GQ and HQ, whereas the U LCa treatment resulted in 0.5% calcite in GQ and HQ. These results evidenced that for GQ and HQ soils an increase in soil carbonation occurred with increasing calcium content in treatment solution. This was not the case for GLA where only U HCa 2S treatment produced quantifiable carbonation levels. These results further confirmed successful MICP by autochthonous indigenous microorganisms on the three soils studied and demonstrated soil carbonation was maximised with the U HCa 2S treatment.

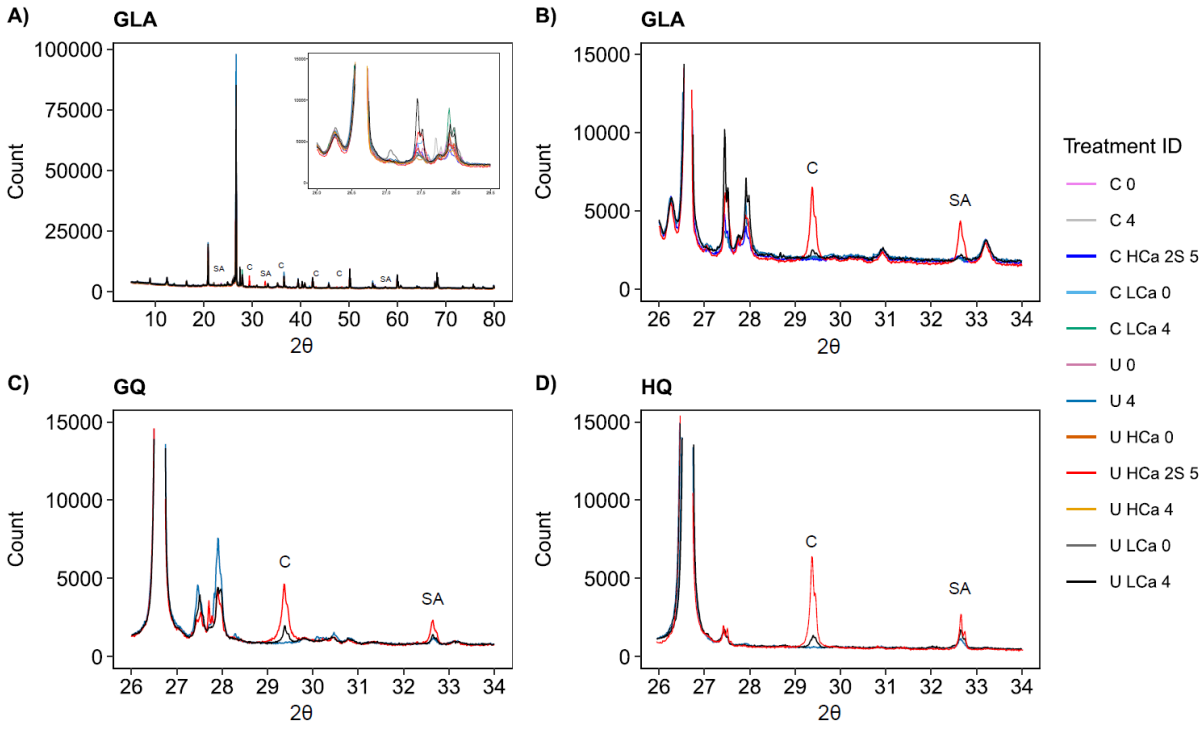


409

410 **Figure 3 XRD analysis of samples following biostimulation of MICP on a-b) GLA, c) GQ and d) HQ soils.**
411 **Legend indicates treatment ID (C, C HCa 2S, C LCa, U, U HCa, U HCa 2S, U LCa) and reaction time ("0",**
412 **"4", "5" refer to $t_r$ = 1 h, 4 and 5 d, respectively). Within plots, C stands for calcite and SA for**
413 **salammoniac.**

414 The thermogravimetric analysis of GLA soil samples is presented in Figure 4a-c and results of GQ
415 and HQ samples in Figure 4e-f. Samples of GLA soil that received control treatments (C, C LCa and
416 C HCa) decomposed in four main stages, i.e., 30-120, 120-390, 390-750 and 750-1100°C, with total
417 weight loss ranging between 7.3 and 10% (Figure 4a-c). Within 120-390°C, the maximum weight loss
418 rate temperature peak determined at 235-238°C coincided with the weight loss rate of nutrient broth
419 (233.7±0.7, wt. = 10.8±0.1%, n = 3) and the peak determined 286-315°C with nutrient broth
420 (323±3.74°C, wt. = 56.3±0.1, n = 3) and ammonium chloride (309±4.75°C, wt. = 95.5±0.2%, n = 3)
421 (Figure S 8). The total weight loss of control samples increased with calcium content, from 7.25±0.06-
422 7.4±0.3 for C to 7.9-8.3% for C LCa and 9.6-10% for C HCa, with increases observed within 30-120
423 and 390-750°C. The relative increases with respect to C (Δwt. = 0.5-0.65% and 2.4-2.7%,
424 respectively) correlated well with theoretical relative weight increases associated to mass of applied
425 calcium (i.e., 0.4% and 2.7% for 50 mM and 333 mM $Ca^{2+}$, respectively).

426 In line with XRD results, samples C, C LCa and U HCa showed identical signatures at $t_0$ and $t_{end}$
427 (Figure 4a-c), indicating no changes due to the applied chemical compounds (e.g., nutrient broth,
428 $NH_4Cl$, urea) occurred over time. In particular for U HCa (Figure 4c), the two peaks observed in
429 control samples (235-238°C and 286-315°C) merged into a single peak between 210-232°C which
430 coincided with the maximum decomposition rate of urea (238.2±1.0°C, wt. = 69.1±0.4%, n = 3) and
431 nutrient broth (Figure S 8). The evolution of urea hydrolysis was observable in GLA soil samples
432 treated with U and U LCa treatments (Figure 4a and c, respectively). At $T_{peak,urea}$ = 238°C, the weight

loss rate of $t_0$ ($t_r$ = 1 h) and $t_1$ ($t_r$ =1 d) samples was greater than their respective controls, indicating presence of urea, whilst at $t_{end}$ ($t_r$ = 4 d) no differences with controls were appreciable indicating all urea had been hydrolysed. The same pattern could be observed for these treatments in GQ and HQ soils at $T_{peak}$ = 238ºC (Figure 4e-f). These results indicated $T_{peak,urea}$ = 238°C could potentially be used to quantify the amount of urea hydrolysed and further confirmed that urea hydrolysis treatment was inhibited for the U HCa treatment (Figure 4b). In U and U LCa treatments, a peak was identified between 192-202°C at $t_0$ and $t_1$ that was not further observable at $t_{end}$ (Figure 4a and c). This peak was not observable in controls, U HCa, nor the chemicals that composed treatment solutions (Figure S 8). The peak fell within the main decomposition temperature of $CaCl_2$ (150-200ºC) however, the fact that no such peak could be observed in U HCa (Figure 4b) indicated it was likely associated with either an intermediate decomposition product or a by-product of urea hydrolysis rather than to $CaCl_2$.

The similar signal of U and U HCa 2S samples at T = 238ºC on day 1 and 5, respectively, indicated most of the applied urea on day 4 had not hydrolysed by day 5 (Figure 4d-f). Presumably, urea hydrolysis was inhibited by the high calcium dose, as observed with U HCa treatment (Figure 4b). The inhibition of urea hydrolysis during the second stage could have implications regarding treatment efficiency. On the one hand, urea in the second stage might have been applied unnecessarily, repercussing treatment costs and sustainability. On the other hand, it implies that the precipitated inorganic carbon was produced during the initial urea application. This would reduce the overall carbonation potential since, during treatment solution replacement, dissolved inorganic carbon from the initial urea application would have been partially removed. In this regard, one stage treatments, application of calcium solely, or applying calcium at doses that allow continuation of urea hydrolysis could improve treatment efficiency.

U HCa 2S GLA samples (Figure 4d) decomposed in six main stages, i.e., 30-120, 120-372, 372-556, 556-737, 737-900, and 900-1100°C with total weight loss of 11.4±0.9%. Five new peaks were identified, with maximum decomposition rates determined at 182±2°C, 575±5, 651±6°C, 785±4°C and 909±4 (n = 6, ± is 1sd), which were not observable in other GLA samples nor chemicals (Figure S 8). The peaks within 100-200, 600-700 and 750-900°C were also detected in GQ and HQ soil samples treated with U HCa 2S and U LCa treatment at $t_{end}$ (Figure 4e-f), indicating a relationship with urea hydrolysis and/or MICP. The observed peaks in GLA, GQ and HQ samples within 750-900°C fell within the well documented thermal decomposition range of calcium carbonate (750-900ºC) (Manning et al., 2005; Galan et al., 2013; Karunadasa et al., 2019). Although speculative, the additional identified peaks could be related to other carbonate products. Amorphous calcium carbonate has been reported to lose weight gradually from 550°C onwards during conversion of $CaCO_3{\cdot}H_2O$ to CaO instead of exhibiting the sharp peak of calcite between 750-900ºC (Ihli et al., 2014). This could explain observed peaks in GLA soil at 575 and 651°C with U HCa 2S and between 600-700°C in GQ and HQ soils with U HCa 2S and U LCa treatments. Non-calcium-based carbonates have been reported to decompose at both lower and higher temperatures than calcite. In particular, cerussite ($PbCO_3$) maximum decomposition rate is reported at 189-199°C (Galwey, 1999) and ammonium carbonate salt ($NH_4CO_3$) decomposes in one stage within 100-200ºC with $T_{peak}$ = 140-160ºC (Zelenková and Slovák,

2022). These could explain the unidentified peaks observed in GLA, GQ and HQ soils with U HCa 2S <200°C. Smithsonite ($ZnCO_3$) decomposes in one stage with maximum decomposition rate determined at 265°C (Liu et al., 2004). Rhodochrosite ($MgCO_3$) decomposes in three stages, with peaks at 580, 665 and 900°C (Reyes et al., 2020), similar to the 575, 651 and 909°C peaks identified in GLA soil. Finally, both witherite ($BaCO_3$) and strontianite ($SrCO_3$), have been reported to decompose in two stages, with peaks occurring at 805 and 963°C (Arvanitidis et al., 1996) and 875°C and 1010°C (Ptáček et al., 2015), respectively.

The calcium carbonate content induced by U HCa 2S treatment in GLA soil estimated from weight loss within 750-900ºC was of 3.2%. Assuming weight losses within 550-750ºC were related to amorphous calcium carbonate precipitation, the total estimated content from TG was 7.2% which was in close agreement with the 6.9% estimated from XRD analysis. Similarly, the estimated calcium carbonate content of GQ and HQ soils within 700-900ºC induced by the U HCa 2S treatment was of 0.5 and 0.6%, respectively, and adding the 550-700 ºC region, 4.2 and 7.3%. This indicated a good agreement between estimation of calcium carbonate minerals of TG and XRD analysis for GQ soil (3.1%) but an overestimation for HQ soil (4.6%). The overestimation of TG analysis which could be related to overlapping decomposition of amorphous calcium carbonate (>550ºC) and structural water mass loss of kaolinite which occurs between 450-700ºC (Ptáček et al., 2011). The carbonate content induced by the U LCa treatment estimated from the 550-700ºC region was 0.64 and 0.71% for GQ and HQ, respectively, coherent with the 0.5% estimated from XRD analysis.

In summary, XRD and TG analyses evidenced the U HCa 2S treatment resulted in calcite precipitation in the three soils studied, U LCa resulted in calcite precipitation in GQ and HQ only, while the U treatment did not result in carbonate precipitation in any of the tested soils. No definite evidence of carbonate minerals other than calcite could be found, and TG data suggested part of precipitated calcium carbonate was amorphous calcium carbonate. Both XRD and TG confirmed soil carbonation was maximised with the U HCa 2S treatment.

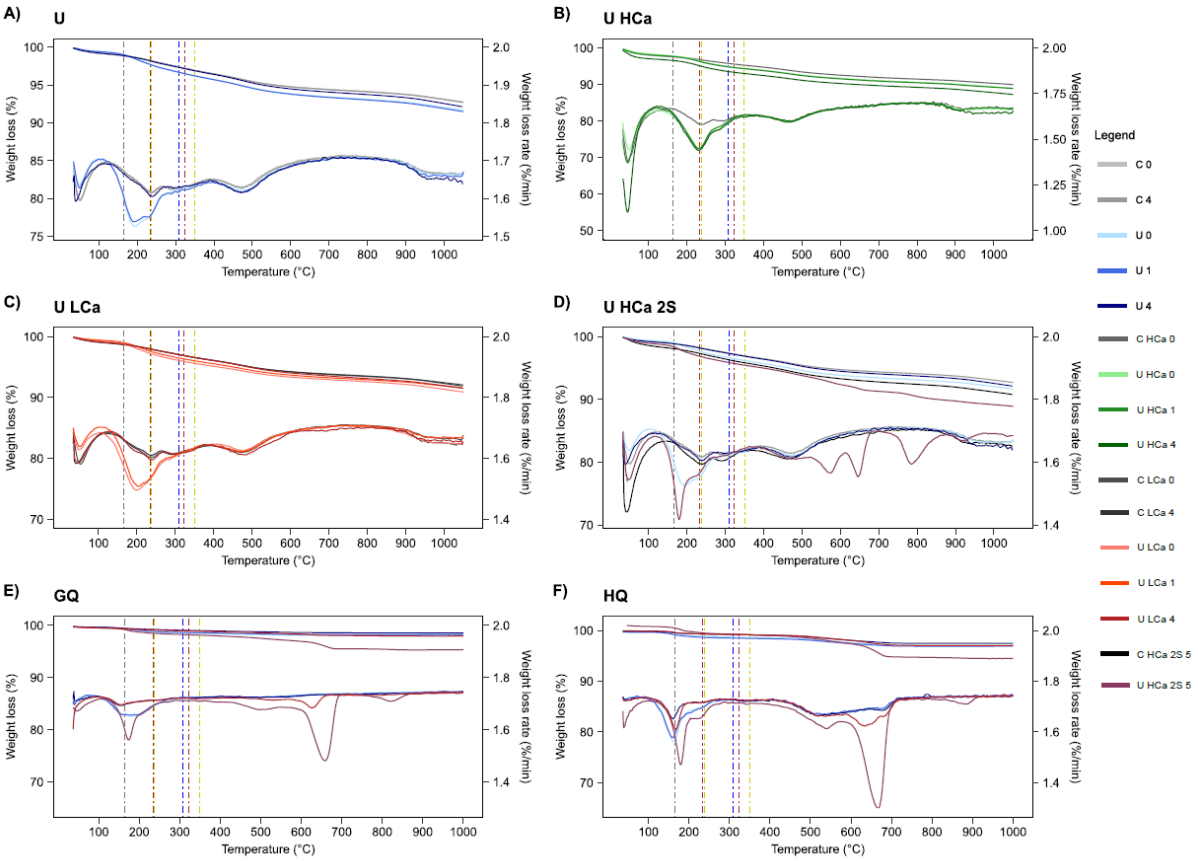


**Figure 4 Thermogravimetric analysis of soil samples throughout biostimulation of MICP: figures a-d) show GLA soil samples that received a specific treatment at various reaction time points; figures e) GQ, and f) HQ, compile several treatments at specific reaction time points. Line colours indicate treatment ID (C, C HCa 2S, C LCa, U, U HCa, U HCa 2S, U LCa) and reaction time ("0", "1", "4", "5" refer to $t_r$ = 1 h, 1, 4 and 5 d, respectively).**

### 3.4. Mineralisation of heavy metals

Relevant elements in the exchangeable fraction of treated GLA soil samples were Al, Ba, Mn, Pb, Sr and Zn (<2 mM) and the other elements that measured (As, Cd, Co, Cr, Cu, Mo, Ni, Sb and V) were in trace concentrations (<0.3 mM) (Figure S 7). This indicated elements present in the total soil fraction (e.g., Cr, V) did not mobilise into the exchangeable fraction as a result of the biogeochemical changes induced by treatments. Subsequent data analysis thus focused on Al, Ba, Mn, Pb, Sr and Zn.

#### 3.4.1. Elements' behaviour in response to treatment

Element's behaviour in the soil exchangeable (Figure 5) and carbonate (Figure 6) fractions in response to treatment were analysed through a non-targeted hierarchical cluster analysis (HCA). Samples in the exchangeable fraction grouped into five clusters which could be associated to specific treatments inducing different soil environmental conditions (Figure 5). The control treatments and the early time points ($t_r$ ≤1 d), in which urea hydrolysis might have not been significant yet, appeared in two clusters. These were a) controls with $Ca^{2+}$ ≤50 mM and U samples at t= 1 h ($t_0$) and b) controls without and with calcium (C, C LCa, C HCa 2S) at $t_{end}$ ($t_r$ = 4 or 5 d) plus U LCa samples at $t_r$ ≤1 d. $t_0$

517 and $t_{end}$ in control samples clustered in two different groups indicating an effect of time on the samples
518 even urea hydrolysis or MICP treatment. Samples treated with U at $t_r$ = 1 and 4 d formed a cluster
519 indicating a specific effect of urea hydrolysis that happened rapidly. Samples that underwent inhibition
520 of urea hydrolysis by U HCa ($t_0$ to $t_{end}$) formed another cluster. Finally, samples that underwent urea
521 hydrolysis where calcium was available (U LCa and U HCa 2S treatments at $t_{end}$) formed a
522 differentiated cluster indicating specific effect of urea hydrolysis in the presence of $Ca^{2+}$ potentially
523 related to MICP.

524 Elements in the exchangeable fraction grouped as Sr-Mn, Pb-Zn and Al-Ba. The Pb and Zn profiles in
525 the exchangeable fraction were nearly identical. The highest values were observed where urea
526 hydrolysis was insignificant (controls, short reaction time ≤1 d) or inhibited (U HCa). Lower values
527 were observed in samples that underwent urea hydrolysis, and the lowest values in samples that
528 underwent urea hydrolysis in the presence of calcium (i.e., U LCa and U HCa 2S). For Mn and Sr,
529 instead, higher values were observed in samples that underwent urea hydrolysis (U) and where urea
530 hydrolysis was inhibited by high calcium dose (U HCa). Of the samples that underwent urea
531 hydrolysis, only samples that underwent significant MICP showed low values of Mn and Sr (i.e., U
532 HCa 2S). Al and Ba generally showed higher values in control and urea treatments that excluded
533 calcium at early time points (1 h).

534 In the carbonate fraction, elements Ba, Mn, Sr, Pb and Zn formed a cluster whereas Al formed its own
535 cluster (Figure 6). The HCA aggregated samples into four groups which reflected a) controls with and
536 without calcium; b) treatments containing urea where urea hydrolysis was insignificant due to short
537 reaction times (U and U LCa, $t_r$ ≤1 d) or inhibition (U HCa); c) samples where urea hydrolysis was
538 significant and either no calcium or low calcium was present (U and U LCa at $t_{end}$) and d) samples that
539 underwent MICP (U HCa 2S at $t_{end}$). Notably, U HCa 2S induced a marked increase in carbonate
540 bound Pb, Zn, Sr, Ba and Mn compared to other treatments. Samples that underwent urea hydrolysis
541 in absence (U) and presence of low calcium (U LCa) also induced increases of Sr, Ba, Mn and Zn in
542 the carbonate fraction, where presence of calcium resulted in higher increases.

543 Overall, the HCA evidenced elements in the exchangeable fraction did not respond equally to the
544 applied treatments. The HCA indicated that Pb and Zn behaviour was strongly linked to urea
545 hydrolysis and MICP, indicating potential removal from the exchangeable fraction. This was less
546 evident for Mn, Sr and Ba, whereas Al appreared to behave particularly independently. In the
547 carbonate fraction, the HCA evidenced a much more homogeneous response in elements behaviour
548 to samples that underwent MICP, indicating carbonation of all elements except Al.

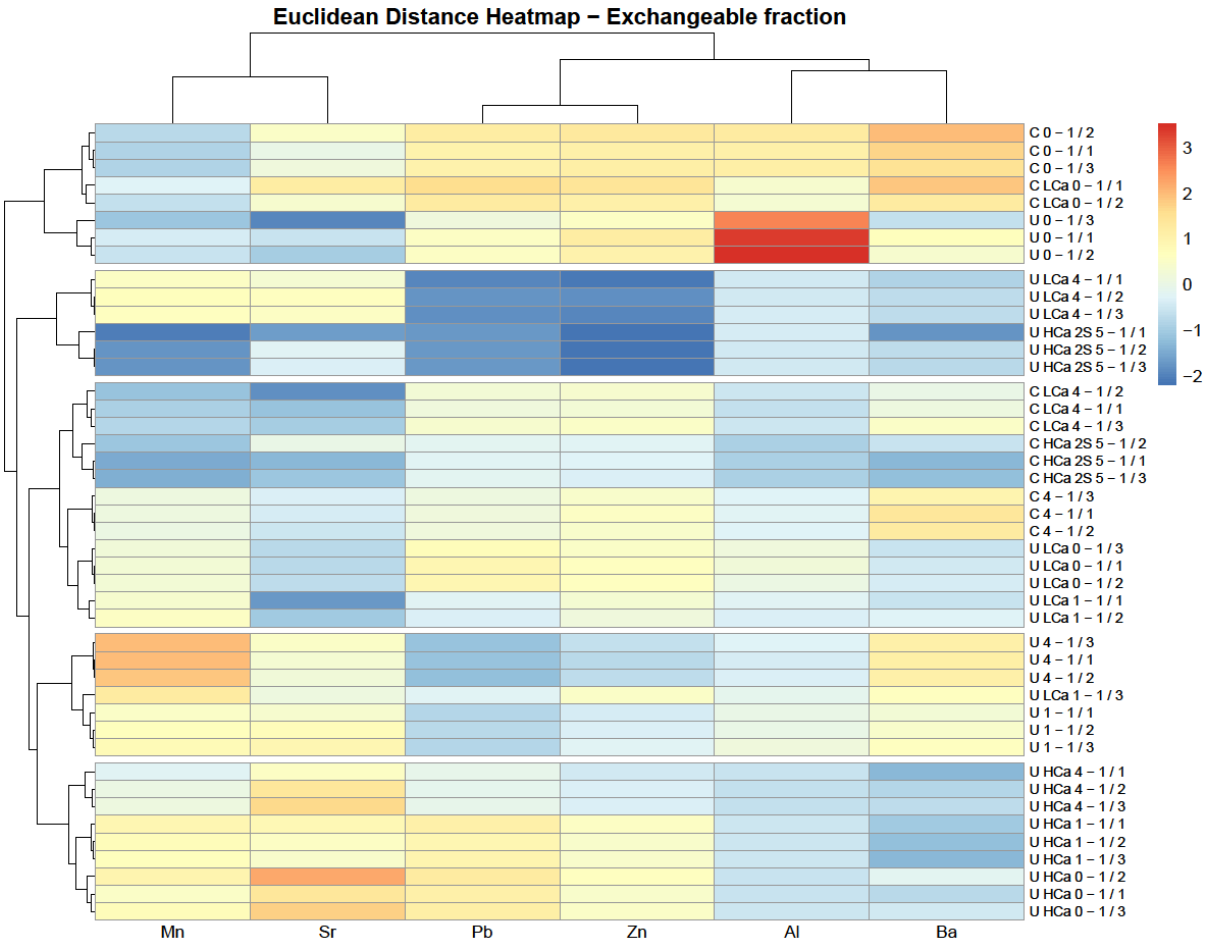


**Figure 5 Euclidean distance heatmap of hierarchical cluster analysis (HCA) of element concentrations determined by ICP-OES on soil carbonate (bottom) fraction. Sample ID's are organised as: Treatment ID (e.g., "C" for Control), time point (e.g., "4" or 4 days), soil fraction (i.e., 1 = exchangeable, 2 = carbonate) and sample replicate (e.g., /1, replicate 1).**

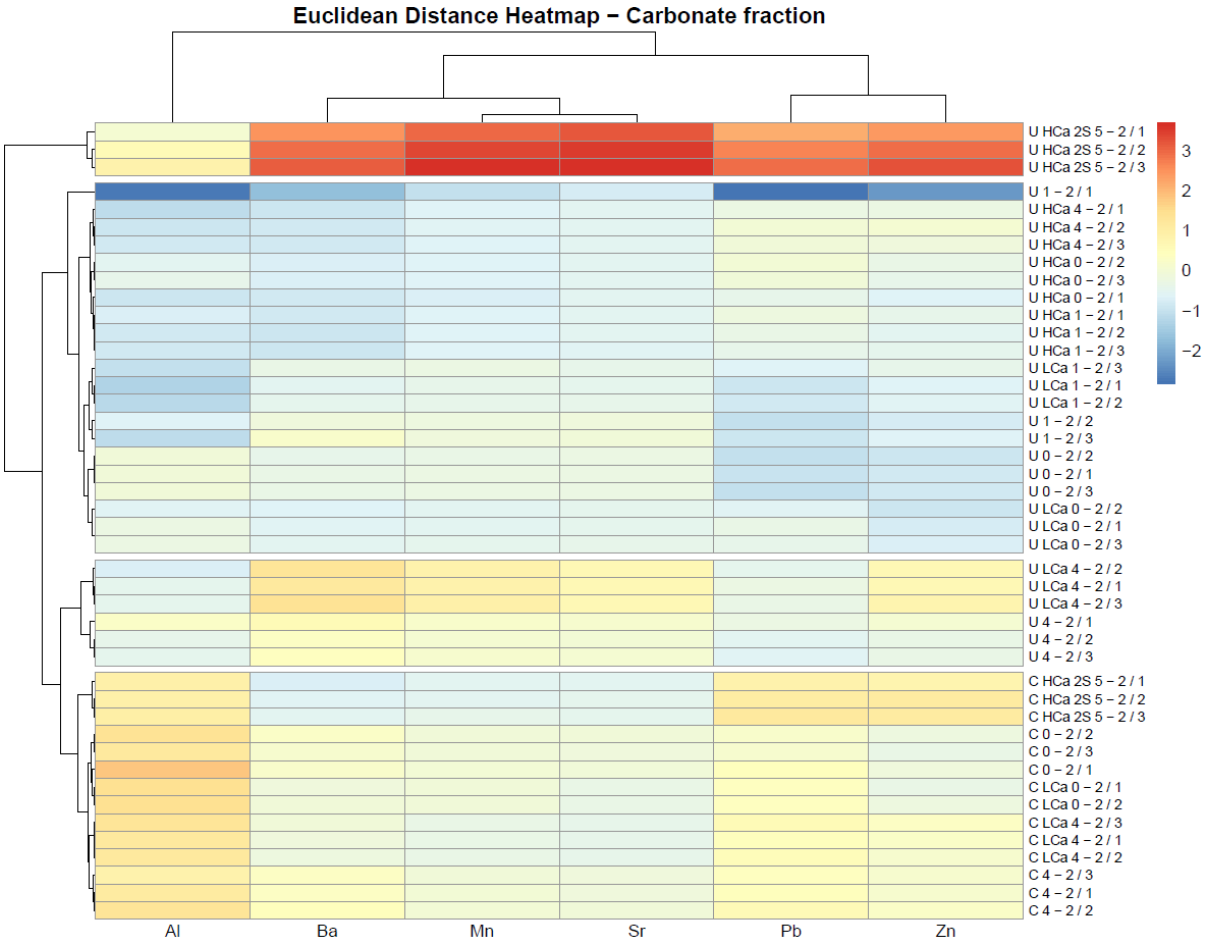


**Figure 6 Euclidean distance heatmap of hierarchical cluster analysis (HCA) of element concentrations determined by ICP-OES on soil carbonate (bottom) fraction. Sample ID's are organised as: Treatment ID (e.g., "C" for Control), time point (e.g., "4" or 4 days), soil fraction (i.e., 1 = exchangeable, 2 = carbonate) and sample replicate (e.g., /1, replicate 1).**

### 3.4.2. Removal efficiency through soil carbonation

The quantitative element removal efficiency of each treatment relative to control (C) at $t_0$ ($t_r$ = 1 h) is presented in Figure 7. All treatments consistently removed Pb (25-93%) and Zn (20-98%) from the exchangeable fraction (Figure 7a-b). Significantly larger removals were quantified in samples that underwent urea hydrolysis in absence (U, 71 and 55% for Pb and Zn, respectively) and presence of calcium (U LCa and U HCa 2S, 88-93% and 91-98%, respectively) compared to controls (25-40% and 20-46%). Among the samples that underwent urea hydrolysis, the results confirmed that the presence of calcium enhanced removal of Pb and Zn from the exchangeable fraction; also observed by Liu et al. (2021) in bioaugmentation experiments on mine tailings containing Pb and Zn. Removal of Pb and Zn from the exchangeable fraction with urea hydrolysis at $Ca^{2+}$ <50 mM (U and U LCa), however, did not translate in significant increases in the carbonate fraction. For Pb removal (20-24%) was observed instead. For Zn, urea hydrolysis per se (U) did not result in changes in the carbonate fraction and, despite in the presence of 50 mM $Ca^{2+}$ Zn partition into the carbonate fraction occurred (U LCa, 45%), it was within increases induced by control treatments (19-59%) (Figure 7b). The highest Pb and Zn partition into the carbonate fraction occurred in samples that underwent MICP (U HCa 2S), consistent

with observations of bioaugmentation studies on soils and mine tailings (Achal et al., 2012b; Govarthanan et al., 2013; Yang et al., 2016; Liu et al., 2021). Removal of Pb from the carbonate fraction at $Ca^{2+}$ ≤50 mM was somewhat surprising, since Pb carbonation has been documented both via urea hydrolysis (Yang et al., 2016) and MICP at calcium concentrations of 25 mM (Achal et al., 2012b; Yang et al., 2016). An increase of Pb in the oxyhydroxide fraction was observed with U LCa (25%), indicating potential precipitation as lead hydroxide ($Pb(OH)_2$) in treatments that induced a high pH as a result of urea hydrolysis (i.e., U and U LCa). Partition of Pb into the oxyhydroxide fraction, however, has not been observed in bioremediation studies (Achal et al., 2012b; Govarthanan et al., 2013; Yang et al., 2016; Liu et al., 2021). With lead solubility being minimum within 8< pH <11, the stable forms of Pb in aqueous systems within 6< pH <8.3 comprise cerussite ($PbCO_3$) and hydro-cerrusite [$Pb(OH)_2(CO_3)_2$] whilst lead hydroxide [$Pb(OH)_2$] is most stable at pH >8.3 (Hem et al., 1973). Therefore, it is possible that the lower pH induced by MICP (U HCa 2S $t_{end}$ pH = 8.4) compared to U and U LCa (pH = 9) (Figure 2) favoured Pb partition into the carbonate fraction rather than the oxyhydroxide fraction and *vice versa*.

Removal of Mn and Sr from the exchangeable fraction only occurred with controls that contained calcium and samples that underwent MICP (Figure 7c-d). In the case of Mn, a significantly higher removal occurred with MICP (U HCa 2S, 39%) compared to controls (5 and 20% with LCa and HCa, respectively). Urea hydrolysis at $Ca^{2+}$ <50 Mm induced mobilisation of Mn in the exchangeable fraction, which was lower in the presence of calcium (U LCa, 53%) than in its absence (U, 103%) and could have mobilised from the organic matter fraction (Figure 7c). Mn is a very reactive element in the soil environment which forms complexes with organic matter and is sensitive to changes in redox, pH and microbial activity (for a review see Li et al., 2021). In alkaline conditions, Mn solubility is typically low however, reducing conditions such as those that occur in waterlogged soils can trigger dissolution of Mn-organic matter complexes (Grybos et al., 2009), which may have occurred due to excess water. Furthermore, increases in soil solution pH can lead to increased soil organic matter dissolution into water (Evans et al., 2012), which could have occurred with GLA samples (TC = 3%) that underwent urea hydrolysis. Except for the mobilisation from the organic matter fraction, Sr followed the same patterns as Mn however, changes in Sr were generally small (2-20%) and not significantly different than controls (Figure 7d). Samples that underwent MICP experienced a large increase in Mn and Sr partition into the carbonate fraction. Urea hydrolysis at $Ca^{2+}$ <50 mM also resulted in relative increases, which were higher with calcium (92-109%) than without (19-20%). Thus, the data indicated that Mn and Sr partition into the carbonate fraction resulted from urea hydrolysis and increased with increasing calcium content. Similar results for Sr following bioaugmentation of an aquifer sand were reported by Achal et al. (2012c), while no studies have been found for Mn. Decreases in the carbonate fraction of Mn and Sr were recorded in the absence of urea hydrolysis and presence of calcium (28-64%).

The behaviour of Ba in the exchangeable fraction had similarities Pb and Zn in that all treatments resulted in removal (6.7-35%) (Figure 7e). Samples that received calcium showed similar (C LCa, C HCa 2S, U LCa, U HCa 2S, 19-35%) and higher removal than those that did not (C, U, 6.7-7.9%),

613 independently of calcium content or urea hydrolysis. In the carbonate fraction, Ba showed a similar
614 response to Mn and Sr, in that urea hydrolysis without (U, 13%), with low calcium (U LCa, 58%) and
615 MICP (U HCa 2S, 142%) increased Ba partition into the carbonate fraction, and control treatments
616 that contained calcium resulted in removal. Furthermore, data indicated Ba could have mobilised from
617 both the organic matter (37%) and the oxyhydroxide (26%) soil fractions as a result of high calcium
618 content. To our knowledge, no studies have been conducted on Ba in the context of MICP. Similar to
619 Pb, Zn and Ba, all treatments removed Al from the exchangeable fraction (61-89%) (Figure 7e).
620 Removal from the carbonate fraction was also recorded (5-57%), which was larger in samples that
621 contained urea or underwent urea hydrolysis in the absence and presence low calcium (U, U LCa, U
622 HCa, 40-57%) than controls (5-12%). In comparison to U, U LCa and U HCa, a lower removal was
623 observed samples that underwent MICP (U HCa 2S, 22%). Changes in the rest of soil fractions
624 presented significant variability across samples and the results were thus inconclusive. Notably, Al
625 was the only element for which the concentration did not increase in the carbonate fraction with MICP.
626 Between pH of 7 and 9, Al precipitates out of solution as gibbsite, $Al(OH)_3$, (Brautigan et al., 2012) and
627 may explain the observed changes in Al.

628 Overall, the results of the sequential extraction demonstrated MICP maximised partition of Pb, Zn,
629 Mn, Sr, Ba into the carbonate fraction. Furthermore, MICP was most effective in removing Pb and Zn
630 from the exchangeable fraction. Zn, Mn, Sr and Ba partition into the carbonate fraction increased with
631 increasing calcium content. However, results indicated urea hydrolysis at $Ca^{2+}$ <50 mM resulted in Pb
632 partition into the oxyhydroxide fraction and mobilisation of Mn which may have been related to the
633 higher pH observed in these samples compared to MICP. Al did not participate in carbonation and
634 appeared to behave independently of urea hydrolysis and/or MICP.

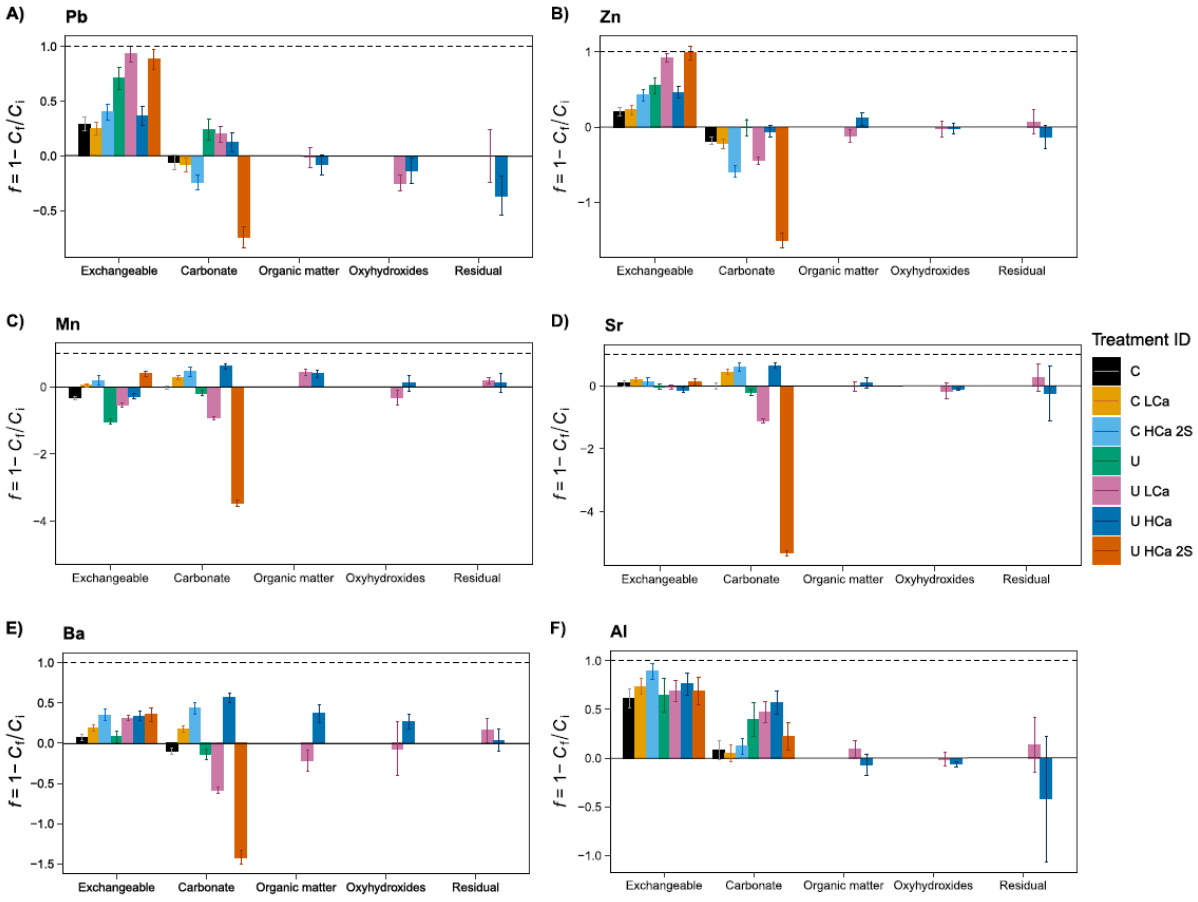


**Figure 7 Normalised element fractionation at $t_{end}$ relative to control (C, $t_0$) of Pb, Zn, Mn, Ba, Al and Sr in exchangeable, carbonate, organic matter (OM), oxyhydroxide and residual soil fractions of GLA soil with different treatments. Bars and error bars indicate average and standard error of three replicate samples calculated as indicated in (7).**

## 4. Conclusions

This study investigated the simultaneous bioremediation of multiple heavy metals through the biostimulation of soils' autochthonous ureolytic bacteria at varying calcium-to-urea ratios. The effect of varying calcium-to-urea ratio was evaluated with the aim of maximising element immobilisation and carbon sequestration through soil carbonation. The selected calcium-to-urea ratios covered a range of scenarios in which MICP may occur, namely urea application in agricultural settings, environmental bioremediation of heavy metals, and enhancement of soil mechanical properties in engineering contexts.

The results of this study highlighted comparable urea hydrolysis and MICP by autochthonous ureolytic bacteria from a vacant and derelict land site from Glasgow containing 5-7 times Pb, Zn, Mn, Sr, Ba and Al compared to background levels determined in two regional soils. Urea hydrolysis on the tested soils was similarly affected by the calcium-to-urea ratio, such that delay to inhibition of urea hydrolysis occurred with 50 mM and 333 mM $Ca^{2+}$, respectively. Application of urea and 333 mM $Ca^{2+}$ in a second step following an initial application of urea induced significant MICP. However, results

indicated urea hydrolysis during the second step was inhibited by the high calcium dose and thus the precipitated carbonates originated from the initial application of urea. A two-step treatment could be less efficient than one-step treatments in terms of costs and sustainability and further research is needed to determine minimum calcium concentrations tolerable by soil indigenous ureolytic bacteria.

Elements' behaviour and soil carbonation were also affected by the calcium-to-urea ratio. Carbon sequestration through mineral trapping and element immobilisation in the carbonate fraction were maximised with the two-step treatment at equimolar calcium-to-urea ratio of 333 mM. This approach resulted in a ~7% increase in the soil carbonate content and removal of >85% of Pb and Zn from the exchangeable fraction, along with the highest Mn, Ba, Sr, and Ba partition into the carbonate fraction. Newly formed calcite was evidenced by XRD, indicating incorporation of elements into the calcite mineral structure, and TG indicated part of the precipitated calcium carbonate was amorphous.
A lower calcium-to-urea ratio (50:333 mM) also induced high removal of Pb and Zn from the exchangeable fraction but resulted in significantly less partition of Zn, Sr, Ba and Mn into the soil carbonate fraction and low soil carbonate content (0-0.7%). Importantly, at $Ca^{2+}$ ≤50 mM Pb partitioned into the oxyhydroxide fraction. This was attributed to the higher stability of $Pb(OH)_2$ at the pH induced by urea hydrolysis at $Ca^{2+}$ ≤50 mM. The soil oxyhydroxide fraction could be a labile pool and therefore not constitute a stable form of bioremediation.
In absence of calcium, urea hydrolysis increased minimally the carbonate bound Sr, Mn and Ba and resulted in insignificant partition of Pb and Zn into the carbonate fraction. No detectable levels of carbonate products could be identified. In addition, Mn from the organic matter fraction mobilised into the exchangeable fraction, which could be linked to the solubilisation of organic matter due to the high pH induced by urea hydrolysis and/or changes in redox conditions caused by microbial activity.

The results of this study highlight the potential of soil's autochthonous ureolytic bacteria for the bioremediation of heavy metals through MICP. Furthermore, it establishes a precedence of multiple element immobilisation and differing immobilisation mechanisms which were element and treatment dependant. Based on the presented results, we recommend a two-step treatment with equimolar urea-to-calcium ratio of 333 mM to maximise carbon sequestration and element partition into the carbonate fraction in the context of bioremediation via MICP.

## Acknowledgements

Special thanks are given to the funding body UKRI Natural Environment Research Council, A. Hunter, E. Palmer, Dr C. Brolly, Dr C. Wilson, Dr L. Spruzeniece, K. Roberts and Dr M. Wildman of the University of Glasgow, Dr V. Olive and Dr G. MacKinnon of the Scottish Universities Environmental Research Centre (SUERC), E. Murray of the GALLANT research project, J. King of Hugh King Tillicoultry Quarries, and J. Duckett of the Glasgow City Council for their support.

## Funding sources

This work was supported by the UK Research and Innovation Natural Environment Research Council [grant number NE/W005042/1].

## References


Achal, V., Pan, X. and Zhang, D., 2011. Remediation of copper-contaminated soil by Kocuria flava CR1, based on microbially induced calcite precipitation. Ecological Engineering, 37(10), pp.1601-1605. https://doi.org/10.1016/j.ecoleng.2011.06.008

Achal, V., Pan, X., Fu, Q. and Zhang, D., 2012a. Biomineralization based remediation of As (III) contaminated soil by Sporosarcina ginsengisoli. Journal of hazardous materials, 201, pp.178-184. https://doi.org/10.1016/j.jhazmat.2011.11.067

Achal, V., Pan, X., Zhang, D. and Fu, Q., 2012b. Bioremediation of Pb-contaminated soil based on microbially induced calcite precipitation. J Microbiol Biotechnol, 22(2), pp.244-7. https://doi.org/10.4014/jmb.1108.08033

Achal, V., Pan, X. and Zhang, D., 2012c. Bioremediation of strontium (Sr) contaminated aquifer quartz sand based on carbonate precipitation induced by Sr resistant Halomonas sp. Chemosphere, 89(6), pp.764-768. https://doi.org/10.1016/j.chemosphere.2012.06.064

Achal, V., Pan, X., Lee, D.J., Kumari, D. and Zhang, D., 2013. Remediation of Cr (VI) from chromium slag by biocementation. Chemosphere, 93(7), pp.1352-1358. https://doi.org/10.1016/j.chemosphere.2013.08.008

Achal, V. and Pan, X., 2014. Influence of calcium sources on microbially induced calcium carbonate precipitation by Bacillus sp. CR2. Applied biochemistry and biotechnology, 173, pp.307-317. https://doi.org/10.1007/s12010-014-0842-1

Al Qabany, A., Soga, K. and Santamarina, C., 2012. Factors affecting efficiency of microbially induced calcite precipitation. Journal of Geotechnical and Geoenvironmental Engineering, 138(8), pp.992-1001. https://doi.org/10.1061/(ASCE)GT.1943-5606.0000666

Al Qabany, A. and Soga, K., 2014. Effect of chemical treatment used in MICP on engineering properties of cemented soils. In Bio-and chemo-mechanical processes in geotechnical engineering: géotechnique symposium in print 2013 (pp. 107-115). ICE Publishing. https://doi.org/10.1680/bcmpge.60531.010

Ali, A., Li, M., Su, J., Li, Y., Wang, Z., Bai, Y., Ali, E.F. and Shaheen, S.M., 2022. Brevundimonas diminuta isolated from mines polluted soil immobilized cadmium (Cd2+) and zinc (Zn2+) through calcium carbonate precipitation: microscopic and spectroscopic investigations. Science of the Total Environment, 813, p.152668. https://doi.org/10.1016/j.scitotenv.2021.152668

Arvanitidis, I., Siche, D. and Seetharaman, S., 1996. A study of the thermal decomposition of BaCO3. Metallurgical and materials transactions B, 27, pp.409-416. https://doi.org/10.1007/BF02914905

Bache, B.W., 1984. The role of calcium in buffering soils. Plant, Cell & Environment, 7(6), pp.391-395. https://doi.org/10.1111/j.1365-3040.1984.tb01428.x

Bai, H., Liu, D., Zheng, W., Ma, L., Yang, S., Cao, J., Lu, X., Wang, H. and Mehta, N., 2021. Microbially-induced calcium carbonate precipitation by a halophilic ureolytic bacterium and its potential for remediation of heavy metal-contaminated saline environments. International Biodeterioration & Biodegradation, 165, p.105311. https://doi.org/10.1016/j.ibiod.2021.105311

Bhattacharya, A., Naik, S.N. and Khare, S.K., 2018. Harnessing the bio-mineralization ability of urease producing Serratia marcescens and Enterobacter cloacae EMB19 for remediation of heavy metal cadmium (II). Journal of Environmental Management, 215, pp.143-152. https://doi.org/10.1016/j.jenvman.2018.03.055

Brautigan, D.J., Rengasamy, P. and Chittleborough, D.J., 2012. Aluminium speciation and phytotoxicity in alkaline soils. Plant and Soil, 360, pp.187-196. https://doi.org/10.1007/s11104-012-1232-5

Burbank, M.B., Weaver, T.J., Williams, B.C. and Crawford, R.L., 2012. Urease activity of ureolytic bacteria isolated from six soils in which calcite was precipitated by indigenous bacteria. Geomicrobiology Journal, 29(4), pp.389-395. https://doi.org/10.1080/01490451.2011.575913

Cardoso, R., Borges, I., Vieira, J., Duarte, S.O. and Monteiro, G.A., 2023. Interactions between clay minerals, bacteria growth and urease activity on biocementation of soils. Applied Clay Science, 240, p.106972. https://doi.org/10.1016/j.clay.2023.106972

Chapter 12 Decomposition of carbonates, 1999. Galwey, A. K., Brown, M. E. (ed) Studies in Physical and Theoretical Chemistry, pp. 345-364. https://doi.org/10.1016/S0167-6881(99)80014-7

Chai, L., Huang, S., Yang, Z., Peng, B., Huang, Y. and Chen, Y., 2009. Cr (VI) remediation by indigenous bacteria in soils contaminated by chromium-containing slag. Journal of Hazardous Materials, 167(1-3), pp.516-522. https://doi.org/10.1016/j.jhazmat.2009.01.030

Chen, X. and Achal, V., 2019. Biostimulation of carbonate precipitation process in soil for copper immobilization. Journal of hazardous materials, 368, pp.705-713. https://doi.org/10.1016/j.jhazmat.2019.01.108

Cheng, L., Shahin, M.A., Cord-Ruwisch, R., Addis, M., Hartanto, T. and Elms, C., 2014. Soil stabilisation by microbial-induced calcite precipitation (MICP): investigation into some physical and environmental aspects. In 7th international congress on environmental geotechnics (Vol. 64, No. 12, pp. 1105-1112). Engineers Australia Melbourne, Australia.

Chung, H., Kim, S.H. and Nam, K., 2020. Inhibition of urea hydrolysis by free Cu concentration of soil solution in microbially induced calcium carbonate precipitation. Science of The Total Environment, 740, p.140194. https://doi.org/10.1016/j.scitotenv.2020.140194

Cui, M.J., Teng, A., Chu, J. and Cao, B., 2022. A quantitative, high-throughput urease activity assay for comparison and rapid screening of ureolytic bacteria. Environmental Research, 208, p.112738. https://doi.org/10.1016/j.envres.2022.112738

de Mendiburu F (2021). _agricolae: Statistical Procedures for Agricultural Research_. R package version 1.3-5, https://CRAN.R-project.org/package=agricolae

Diamond, S. and Kinter, E.B., 1966. Adsorption of calcium hydroxide by montmorillonite and kaolinite. Journal of colloid and interface science, 22(3), pp.240-249. https://doi.org/10.1016/0021-9797(66)90029-4

Do, H., Wang, Y., Long, Z., Ketehouli, T., Li, X., Zhao, Z. and Li, M., 2020. A psychrotolerant Ni-resistant Bacillus cereus D2 induces carbonate precipitation of nickel at low temperature.

Dupraz, S., Parmentier, M., Ménez, B., & Guyot, F. (2009). Experimental and numerical modeling of bacterially induced pH increase and calcite precipitation in saline aquifers. Chemical Geology, 265(1–2), 44–53. https://doi.org/10.1016/j.chemgeo.2009.05.003

Ecotoxicology and Environmental Safety, 198, p.110672. https://doi.org/10.1016/j.ecoenv.2020.110672

Encyclopedia of Global Change. Edited by: David Cuff and Andrew S. Goudie. Publisher: Oxford University PressPrint Publication Date: 2001. Print ISBN-13: 9780195108255. Published online: 2005. Current Online Version: 2005e. ISBN: 9780195187588. https://doi.org/10.1093/acref/9780195108255.001.0001

Evans, C.D., Jones, T.G., Burden, A., Ostle, N., Zieliński, P., Cooper, M.D., Peacock, M., Clark, J.M., Oulehle, F., Cooper, D. and Freeman, C., 2012. Acidity controls on dissolved organic carbon mobility in organic soils. Global Change Biology, 18(11), pp.3317-3331. https://doi.org/10.1111/j.1365-2486.2012.02794.x

Fang, L., Niu, Q., Cheng, L., Jiang, J., Yu, Y.Y., Chu, J., Achal, V. and You, T., 2021. Ca-mediated alleviation of Cd2+ induced toxicity and improved Cd2+ biomineralization by Sporosarcina pasteurii. Science of The Total Environment, 787, p.147627. https://doi.org/10.1016/j.scitotenv.2021.147627

FAO and UNEP. 2021. Global Assessment of Soil Pollution: Report. Rome. https://doi.org/10.4060/cb4894en

Fu, T., Saracho, A.C. and Haigh, S.K., 2023. Microbially induced carbonate precipitation (MICP) for soil strengthening: A comprehensive review. Biogeotechnics, p.100002. https://doi.org/10.1016/j.bgtech.2023.100002

Fujita, Y., Ferris, F.G., Lawson, R.D., Colwell, F.S. and Smith, R.W., 2000. Subscribed content calcium carbonate precipitation by ureolytic subsurface bacteria. Geomicrobiology Journal, 17(4), pp.305-318. https://doi.org/10.1080/782198884

Fujita, Y., Redden, G.D., Ingram, J.C., Cortez, M.M., Ferris, F.G. and Smith, R.W., 2004. Strontium incorporation into calcite generated by bacterial ureolysis. Geochimica et cosmochimica acta, 68(15), pp.3261-3270. https://doi.org/10.1016/j.gca.2003.12.018

Galan, I., Glasser, F.P. and Andrade, C., 2013. Calcium carbonate decomposition. Journal of Thermal Analysis and Calorimetry, 111, pp.1197-1202. https://doi.org/10.1007/s10973-012-2290-x

Gat, D., Ronen, Z. and Tsesarsky, M., 2017. Long-term sustainability of microbial-induced CaCO3 precipitation in aqueous media. Chemosphere, 184, pp.524-531. https://doi.org/10.1016/j.chemosphere.2017.06.015

Gianfreda, L., Rao, M.A. and Violante, A., 1992. Adsorption, activity and kinetic properties of urease on montmorillonite, aluminium hydroxide and AL (OH) x-montmorillonite complexes. Soil Biology and Biochemistry, 24(1), pp.51-58. https://doi.org/10.1016/0038-0717(92)90241-O

Gomez, M.G., Anderson, C.M., Graddy, C.M., DeJong, J.T., Nelson, D.C. and Ginn, T.R., 2017. Large-scale comparison of bioaugmentation and biostimulation approaches for biocementation of sands. Journal of geotechnical and geoenvironmental engineering, 143(5), p.04016124. https://doi.org/10.1061/(ASCE)GT.1943-5606.0001640

Govarthanan, M., Lee, K.J., Cho, M., Kim, J.S., Kamala-Kannan, S. and Oh, B.T., 2013. Significance of autochthonous Bacillus sp. KK1 on biomineralization of lead in mine tailings. Chemosphere, 90(8), pp.2267-2272. https://doi.org/10.1016/j.chemosphere.2012.10.038

Grybos, M., Davranche, M., Gruau, G., Petitjean, P. and Pédrot, M., 2009. Increasing pH drives organic matter solubilization from wetland soils under reducing conditions. Geoderma, 154(1-2), pp.13-19. https://doi.org/10.1016/j.geoderma.2009.09.001

Haynes, W.M. (ed.). CRC Handbook of Chemistry and Physics. 95th Edition. CRC Press LLC, Boca Raton: FL 2014-2015, p. 4-46. https://doi.org/10.1201/9781315380476

He, J., Chen, X., Zhang, Q. and Achal, V., 2019. More effective immobilization of divalent lead than hexavalent chromium through carbonate mineralization by Staphylococcus epidermidis HJ2. International biodeterioration & biodegradation, 140, pp.67-71. https://doi.org/10.1016/j.ibiod.2019.03.012

Helmi, F.M., Elmitwalli, H.R., Elnagdy, S.M. and El-Hagrassy, A.F., 2016. Calcium carbonate precipitation induced by ureolytic bacteria Bacillus licheniformis. Ecological Engineering, 90, pp.367-371. https://doi.org/10.1016/j.ecoleng.2016.01.044

Hem, J.D. and Durum, W.H., 1973. Solubility and occurrence of lead in surface water. Journal (American Water Works Association), pp.562-568. https://www.jstor.org/stable/41267396

Ihli, J., Wong, W.C., Noel, E.H., Kim, Y.Y., Kulak, A.N., Christenson, H.K., Duer, M.J. and Meldrum, F.C., 2014. Dehydration and crystallization of amorphous calcium carbonate in solution and in air. Nature communications, 5(1), p.3169. https://doi.org/10.1038/ncomms4169

Jiang, N.J., Liu, R., Du, Y.J. and Bi, Y.Z., 2019. Microbial induced carbonate precipitation for immobilizing Pb contaminants: Toxic effects on bacterial activity and immobilization efficiency. Science of the Total Environment, 672, pp.722-731. https://doi.org/10.1016/j.scitotenv.2019.03.294

Kang, C.H., Han, S.H., Shin, Y., Oh, S.J. and So, J.S., 2014. Bioremediation of Cd by microbially induced calcite precipitation. Applied biochemistry and biotechnology, 172, pp.2907-2915. https://doi.org/10.1007/s12010-014-0737-1

Kang, C.H., Oh, S.J., Shin, Y., Han, S.H., Nam, I.H. and So, J.S., 2015. Bioremediation of lead by ureolytic bacteria isolated from soil at abandoned metal mines in South Korea. Ecological Engineering, 74, pp.402-407. https://doi.org/10.1016/j.ecoleng.2014.10.009

Karunadasa, K.S., Manoratne, C.H., Pitawala, H.M.T.G.A. and Rajapakse, R.M.G., 2019. Thermal decomposition of calcium carbonate (calcite polymorph) as examined by in-situ high-temperature X-ray powder diffraction. Journal of Physics and Chemistry of solids, 134, pp.21-28. https://doi.org/10.1016/j.jpcs.2019.05.023

Khonje, D.J., Varsa, E.C. and Klubek, B., 1989. The acidulation effects of nitrogenous fertilizers on selected chemical and microbiological properties of soil. Communications in soil science and plant analysis, 20(13-14), pp.1377-1395. https://doi.org/10.1080/00103628909368156

Kim, G., Kim, J. and Youn, H., 2018. Effect of temperature, pH, and reaction duration on microbially induced calcite precipitation. Applied Sciences, 8(8), p.1277. https://doi.org/10.3390/app8081277

Kim, Y., Kwon, S. and Roh, Y., 2021. Effect of divalent cations (Cu, Zn, Pb, Cd, and Sr) on microbially induced calcium carbonate precipitation and mineralogical properties. Frontiers in Microbiology, 12, p.646748. https://doi.org/10.3389/fmicb.2021.646748

Kissel, D.E., Sonon, L., Vendrell, P.F. and Isaac, R.A., 2009. Salt concentration and measurement of soil pH. Communications in Soil Science and Plant Analysis, 40(1-6), pp.179-187. https://doi.org/10.1080/00103620802625377

Kumari, D., Li, M., Pan, X. and Xin-Yi, Q., 2014a. Effect of bacterial treatment on Cr (VI) remediation from soil and subsequent plantation of Pisum sativum. Ecological engineering, 73, pp.404-408. https://doi.org/10.1016/j.ecoleng.2014.09.093

Kumari, D., Pan, X., Lee, D.J. and Achal, V., 2014b. Immobilization of cadmium in soil by microbially induced carbonate precipitation with Exiguobacterium undae at low temperature. International Biodeterioration & Biodegradation, 94, pp.98-102. https://doi.org/10.1016/j.ibiod.2014.07.007

Lapierre, F.M., Schmid, J., Ederer, B., Ihling, N., Büchs, J. and Huber, R., 2020. Revealing nutritional requirements of MICP-relevant Sporosarcina pasteurii DSM33 for growth improvement in chemically defined and complex media. Scientific reports, 10(1), p.22448. https://doi.org/10.1038/s41598-020-79904-9

Li, H., Santos, F., Butler, K. and Herndon, E., 2021. A critical review on the multiple roles of manganese in stabilizing and destabilizing soil organic matter. Environmental science & technology, 55(18), pp.12136-12152. https://doi.org/10.1021/acs.est.1c00299

Li, L., Mao, K., Ippolito, J.A., Xing, W., Chen, X., Zhu, W. and Cheng, Y., 2022. Calcium amendments affect heavy metal bioavailability in acidic and calcareous soils. International Journal of Environmental Science and Technology, pp.1-10. https://doi.org/10.1007/s13762-021-03840-y

Li, M., Cheng, X. and Guo, H., 2013. Heavy metal removal by biomineralization of urease producing bacteria isolated from soil. International Biodeterioration & Biodegradation, 76, pp.81-85. https://doi.org/10.1016/j.ibiod.2012.06.016

Li, M., Cheng, X., Guo, H. and Yang, Z., 2016. Biomineralization of carbonate by Terrabacter tumescens for heavy metal removal and biogrouting applications. Journal of Environmental Engineering, 142(9), p.C4015005. https://doi.org/10.1061/(ASCE)EE.1943-7870.0000970

Liu, P., Zhang, Y., Tang, Q. and Shi, S., 2021. Bioremediation of metal-contaminated soils by microbially-induced carbonate precipitation and its effects on ecotoxicity and long-term stability. Biochemical Engineering Journal, 166, p.107856. https://doi.org/10.1016/j.bej.2020.107856

Liu, Y., Zhao, J., Zhang, H., Zhu, Y. and Wang, Z., 2004. Thermal decomposition of basic zinc carbonate in nitrogen atmosphere. Thermochimica Acta, 414(2), pp.121-123. https://doi.org/10.1016/j.tca.2003.12.004

Lyu, C., Qin, Y., Chen, T., Zhao, Z. and Liu, X., 2022. Microbial induced carbonate precipitation contributes to the fates of Cd and Se in Cd-contaminated seleniferous soils. Journal of hazardous materials, 423, p.126977. https://doi.org/10.1016/j.jhazmat.2021.126977

Manning, D.A.C., Lopez-Capel, E. and Barker, S., 2005. Seeing soil carbon: use of thermal analysis in the characterization of soil C reservoirs of differing stability. Mineralogical Magazine, 69(4), pp.425-435. https://doi.org/10.1180/0026461056940260

Mitchell, J.K. and Santamarina, J.C., 2005. Biological considerations in geotechnical engineering. Journal of geotechnical and geoenvironmental engineering, 131(10), pp.1222-1233. https://doi.org/10.1061/(ASCE)1090-0241(2005)131:10(122

Mortensen, B.M., Haber, M.J., DeJong, J.T., Caslake, L.F. and Nelson, D.C., 2011. Effects of environmental factors on microbial induced calcium carbonate precipitation. Journal of applied microbiology, 111(2), pp.338-349. https://doi.org/10.1111/j.1365-2672.2011.05065.x

Mugwar, A.J. and Harbottle, M.J., 2016. Toxicity effects on metal sequestration by microbially-induced carbonate precipitation. Journal of hazardous materials, 314, pp.237-248. https://doi.org/10.1016/j.jhazmat.2016.04.039

Mwandira, W., Nakashima, K. and Kawasaki, S., 2017. Bioremediation of lead-contaminated mine waste by Pararhodobacter sp. based on the microbially induced calcium carbonate precipitation technique and its effects on strength of coarse and fine grained sand. Ecological engineering, 109, pp.57-64. https://doi.org/10.1016/j.ecoleng.2017.09.011

Petrie, S.E. and Jackson, T.L., 1984. Effects of fertilization on soil solution pH and manganese concentration. Soil Science Society of America Journal, 48(2), pp.315-318. https://doi.org/10.2136/sssaj1984.03615995004800020018x

Proudfoot, D., Brooks, L., Gammons, C.H., Barth, E., Bless, D., Nagisetty, R.M. and Lauchnor, E.G., 2022. Investigating the potential for microbially induced carbonate precipitation to treat mine waste. Journal of hazardous materials, 424, p.127490. https://doi.org/10.1016/j.jhazmat.2021.127490

Ptáček, P., Šoukal, F., Opravil, T., Havlica, J. and Brandštetr, J., 2011. The kinetic analysis of the thermal decomposition of kaolinite by DTG technique. Powder Technology, 208(1), pp.20-25. https://doi.org/10.1016/j.powtec.2010.11.035

Ptáček, P., Bartoníčková, E., Švec, J., Opravil, T., Šoukal, F. and Frajkorová, F., 2015. The kinetics and mechanism of thermal decomposition of SrCO3 polymorphs. Ceramics International, 41(1), pp.115-126. https://doi.org/10.1016/j.ceramint.2014.08.043

Qiao, S., Zeng, G., Wang, X., Dai, C., Sheng, M., Chen, Q., Xu, F. and Xu, H., 2021. Multiple heavy metals immobilization based on microbially induced carbonate precipitation by ureolytic bacteria and the precipitation patterns exploration. Chemosphere, 274, p.129661. https://doi.org/10.1016/j.chemosphere.2021.129661

R Core Team (2022). R: A language and environment for statistical computing. R Foundation for Statistical Computing, Vienna, Austria. URL https://www.R-project.org/

Reyes, I.A., Flores, M., Palacios, E.G., Islas, H., Juárez, J.C., Reyes, M., Teja, A.M. and Pérez, C.A., 2020. Kinetics of the thermal decomposition of rhodochrosite. Minerals, 11(1), p.34. https://doi.org/10.3390/min11010034

Sardar, K., Ali, S., Hameed, S., Afzal, S., Fatima, S., Shakoor, M.B., Bharwana, S.A. and Tauqeer, H.M., 2013. Heavy metals contamination and what are the impacts on living organisms. Greener Journal of Environmental management and public safety, 2(4), pp.172-179.

Song, Y., Kirkwood, N., Maksimović, Č., Zheng, X., O'Connor, D., Jin, Y. and Hou, D., 2019. Nature based solutions for contaminated land remediation and brownfield redevelopment in cities: A review. Science of the Total Environment, 663, pp.568-579. https://doi.org/10.1016/j.scitotenv.2019.01.347

Stabnikov, V., Jian, C., Ivanov, V. and Li, Y., 2013. Halotolerant, alkaliphilic urease-producing bacteria from different climate zones and their application for biocementation of sand. World Journal of Microbiology and Biotechnology, 29, pp.1453-1460. https://doi.org/10.1007/s11274-013-1309-1

Sumner, M.E., 1994. Measurement of soil pH: problems and solutions. Communications in Soil Science and Plant Analysis, 25(7-8), pp.859-879. https://doi.org/10.1080/00103629409369085

Tabatabai, M.A., 1977. Effects of trace elements on urease activity in soils. Soil biology and Biochemistry, 9(1), pp.9-13. https://doi.org/10.1016/0038-0717(77)90054-2

Tessier, A.P.G.C., Campbell, P.G. and Bisson, M.J.A.C., 1979. Sequential extraction procedure for the speciation of particulate trace metals. Analytical chemistry, 51(7), pp.844-851. https://doi.org/10.1021/ac50043a017

UN (2015). Transforming Our World: The 2030 Agenda for Sustainable Development. Resolution Adopted by the General Assembly on 25 September 2015, 42809, 1-13.

Van den Bosch, M. and Sang, Å.O., 2017. Urban natural environments as nature-based solutions for improved public health–A systematic review of reviews. Environmental research, 158, pp.373-384. https://doi.org/10.1016/j.envres.2017.05.040

Wickham, H., ggplot2: Elegant Graphics for Data Analysis. Springer-Verlag New York, 2016.

Xue, Z.F., Cheng, W.C., Wang, L. and Xie, Y.X., 2022. Catalyzing urea hydrolysis using two-step microbial-induced carbonate precipitation for copper immobilization: Perspective of pH regulation. Frontiers in Microbiology, 13, p.1001464. https://doi.org/10.3389/fmicb.2022.1001464

Yang, J., Pan, X., Zhao, C., Mou, S., Achal, V., Al-Misned, F.A., Mortuza, M.G. and Gadd, G.M., 2016. Bioimmobilization of heavy metals in acidic copper mine tailings soil. Geomicrobiology Journal, 33(3-4), pp.261-266. https://doi.org/10.1080/01490451.2015.1068889

Yin, T., Lin, H., Dong, Y., Wei, Z., Li, B., Liu, C. and Chen, X., 2021. Inhibition of cadmium releasing from sulfide tailings into the environment by carbonate-mineralized bacteria. Journal of Hazardous Materials, 419, p.126479. https://doi.org/10.1016/j.jhazmat.2021.126479

Youseif, S.H., Abd El-Megeed, F.H., Humm, E.A., Maymon, M., Mohamed, A.H., Saleh, S.A. and Hirsch, A.M., 2021. Comparative analysis of the cultured and total bacterial community in the wheat rhizosphere microbiome using culture-dependent and culture-independent approaches. Microbiology Spectrum, 9(2), pp.e00678-21. https://doi.org/10.1128/Spectrum.00678-21

Zelenková, G. and Slovák, V., 2022. Decomposition of ammonium salts by quantitative TG-MS. Journal of Thermal Analysis and Calorimetry, 147(24), pp.15059-15068. https://doi.org/10.1007/s10973-022-11747-0

Zeng, Y., Chen, Z., Lyu, Q., Cheng, Y., Huan, C., Jiang, X., Yan, Z. and Tan, Z., 2023. Microbiologically induced calcite precipitation for in situ stabilization of heavy metals contributes to land application of sewage sludge. Journal of Hazardous Materials, 441, p.129866. https://doi.org/10.1016/j.jhazmat.2022.129866

Zhao, Y., Yao, J., Yuan, Z., Wang, T., Zhang, Y. and Wang, F., 2017. Bioremediation of Cd by strain GZ-22 isolated from mine soil based on biosorption and microbially induced carbonate precipitation. Environmental Science and Pollution Research, 24, pp.372-380. https://doi.org/10.1007/s11356-016-7810-y

964 Zhao XingQing, Z.X., Wang Min, W.M., Wang Hui, W.H., Tang Ding, T.D., Huang Jian, H.J. and Sun
965 Yu, S.Y., 2019. Study on the remediation of Cd pollution by the biomineralization of urease-producing
966 bacteria. https://doi.org/10.3390/ijerph16020268

967 Zhu, X., Li, W., Zhan, L., Huang, M., Zhang, Q. and Achal, V., 2016. The large-scale process of
968 microbial carbonate precipitation for nickel remediation from an industrial soil. Environmental
969 Pollution, 219, pp.149-155. https://doi.org/10.1016/j.envpol.2016.10.047